USE OF A THERMODYNAMIC ENGINE CYCLE SIMULATION TO STUDY A TURBOCHARGED SPARK-IGNITION ENGINE

A Thesis

by

VAIBHAV J. LAWAND

Submitted to the Office of Graduate Studies of
Texas A&M University
in partial fulfillment of the requirements for the degree of

MASTER OF SCIENCE

December 2009

Major Subject: Mechanical Engineering

USE OF A THERMODYNAMIC ENGINE CYCLE SIMULATION TO STUDY A TURBOCHARGED SPARK-IGNITION ENGINE

A Thesis

by

VAIBHAV J. LAWAND

Submitted to the Office of Graduate Studies of
Texas A&M University
in partial fulfillment of the requirements for the degree of

MASTER OF SCIENCE

Approved by:

Chair of Committee,	Jerald A. Caton
Committee Members,	Yassin A. Hassan
	Timothy J. Jacobs
Head of Department,	Dennis O'Neal

December 2009

Major Subject: Mechanical Engineering

ABSTRACT

Use of a Thermodynamic Engine Cycle Simulation to Study a Turbocharged Spark-ignition Engine. (December 2009)
Vaibhav J. Lawand, B.E. Mechanical Engineering, Mumbai University, India.
Chair of Advisory Committee: Dr. Jerald A. Caton

The second law analysis is a powerful tool for assessing the performance of engines and has been employed for few decades now. Turbocharged diesel engines have been explored in much detail with the help of second law analyses. There is also a need to examine the turbocharged spark-ignition engines in greater detail using second law analyses as they are gaining popularity in high performance and conventional automobiles as well. A thermodynamic simulation was developed in order to investigate the effects of turbocharging on spark-ignition engines from second law perspective. The exergy values associated with the components of the turbocharger along with the engine components were quantified as a percentage of fuel exergy. The exergy balance values indicated that turbocharger does not add considerably to the overall irreversibilities and combustion irreversibility is still the major source of exergy destruction. A comprehensive parametric investigation was also performed to investigate the effects of compression ratio, intercooler effectiveness, etc. for the turbocharged spark-ignition engine over the entire load and speed range. The simulation studies helped in understanding the behavior of turbocharged spark-ignition engine with these parameters.

A simulation study was also performed to compare the turbocharged engine with the naturally aspirated spark-ignition engine. This study examined the engines for operating parameters like bmep and bsfc over the entire speed range and revealed that turbocharging offers higher bmep and lower bsfc values for most of the operating range. In an additional study, these engines were analyzed for the brake thermal

efficiency values at part load. The results indicated that turbocharging offers marginally higher brake thermal efficiency at part loads.

DEDICATION

I would like to dedicate this thesis to my parents and my brother who have made me the person I am. They have always been supportive of my decisions and have always guided me in the right direction when needed. Without their love and support this thesis would not have been possible.

ACKNOWLEDGEMENTS

It gives me a great pleasure to thank those who made this thesis possible. I owe my deepest gratitude to my committee chair, Dr. Jerald Caton. His continuous guidance, encouragement and support at all the levels of this thesis enabled me develop a greater understanding of this subject. Special thanks to him for going through the numerous revisions and making this thesis worth something.

I would also like to thank my committee members, Dr. Timothy Jacobs and Dr. Yassin Hassan, who offered guidance and support. Their cooperation allowed me to finish this work within time.

Finally, I would like to thank Texas A&M University and all my friends who have always inspired me and encouraged me.

NOMENCLATURE

b	specific exergy
b_f	specific flow exergy
B	system total exergy[1]
B_{in}	total exergy into the system
$B_{destroyed}$	total exergy destroyed in the system
B_{fuel}	total exergy of fuel
B_{out}	total exergy out of the system
B_{stored}	total exergy destroyed in the system
h	system enthalpy
m	total cylinder charge mass
m_a	total mass of air
m_f	total mass of fuel
$\dot{Q}$	heat transfer rate to the cylinder gases
r_c	compression ratio
s	specific entropy
T_{wall}	wall temperature
u	specific internal energy
u_b	specific internal energy of unburned zone
v	specific volume

[1] There exist different symbols for system total exergy used by different authors. The current symbol 'B' was selected for convenience purpose only.

V	cylinder volume
P_b	brake power
$W_{c,i}$	indicated work per cycle

Greek and other symbols

θ	instantaneous crank angle
θ_0	crank angle at start of combustion
ϕ	fuel-air equivalence ratio
η	thermal efficiency
$\eta_{f,i}$	indicated fuel conversion efficiency

Abbreviations

AF or A-F	air to fuel mass ratio
bmep	brake mean effective pressure
bsfc	brake specific fuel consumption
CA	crank angle
EGR	exhaust gas recirculation
imep	indicated mean effective pressure
LHV_f	lower heating value of the fuel
MBT	the start of combustion timing which provides ***M***aximum ***B***rake ***T***orque
CR	Compression ratio
BTE	Brake thermal efficiency
ITE	Indicated thermal efficiency

TABLE OF CONTENTS

Page

Page

LIST OF FIGURES

Page

Page

LIST OF TABLES

Page

1. INTRODUCTION

Internal combustion engine cycle simulation models have proved to be very effective in evaluating engine performance and also contributing towards saving time and money. Engine models perform comprehensive analysis of thermodynamic processes in an engine. Modeling an engine is affecting engine research at all levels, from a greater insight into an engine process to identifying the key variables controlling the process [1]. Modeling also saves researchers from endeavors in costly experiments. Models have been successful in predicting engine behavior over a wide range of operating parameters with greater accuracy. Researchers have been using these models for over 40 years now [2].

Initially, the thermodynamic models were based on the first law of thermodynamics or energy analysis [3]. Alternatively, it has also been established that traditional first law analysis cannot provide complete understanding of engine processes. However, the second law analysis identifies the unrecoverable energy associated with the processes[1]. The second law of thermodynamics in conjunction with the first law provides a clear understanding of engine operations[2]. Soon, application of the second law analysis became a powerful tool for thermodynamic cycle simulation. Many studies have effectively applied the second law analysis to compression-ignition engines and spark-ignition engines [3]. The works in the field of second law analysis were primarily focused on the in-cylinder operations and quantifying the useful portion of energy associated with those. Later, researchers included various engine components like turbochargers in their studies. Though second law analysis has been applied to both compression-ignition and spark-ignition engines, compression-ignition engines have been the area of interest for most of the works. Thus, there are many areas in spark-ignition engines which need to be investigated with the help of the second law analysis. The current study presents one such novel concept of analyzing turbocharged spark-ignition engine using the second law analysis.

This thesis follows the style of *Journal of Automobile Engineering.*

In the present work, a second law analysis of turbocharged spark-ignition engines was developed with the help of simulation in order to explore the losses and finding ways to reduce those. The following section illustrates the second law analysis briefly, reviewing the concept of exergy. In order to develop the model for a turbocharger, it is essential to know the working of a turbocharger. Thus, the section following the second law analysis will provide the details about the turbocharger.

1.1 Second law analysis

The methodical understandings of thermodynamic processes in an engine are incomplete without the use of the second law. The first law or energy analysis treats heat and work both as forms of energy and does not give the direction of processes. However, the second law defines quality of energy by its ability to do useful work [4].The second law of thermodynamics is a great tool as it can give the direction of processes, find the ability of a system to do maximum work and find the processes which will destroy the work [2]. This analysis aids in understanding and exploring various inefficiencies associated with the processes. With the reduction in these efficiencies, engines can achieve better performance. The second law introduces a new concept of 'useful work' called exergy. The exergy of a system is its ability to do maximum work [5].

For a system and surroundings, exergy is the maximum amount of useful work which could be obtained from a system if it goes through a reversible process to a thermodynamic state which is in equilibrium with the surroundings[5].Exergy is important as it distinguishes the "available" portion of energy from the "unavailable" portion of energy. Also, it is not a conservative property. Irreversible processes may destroy the exergy. The following section provides details about how to determine exergy for various applications.

Thermodynamic properties are needed to evaluate exergy at a specified set of conditions. Generally, for mobile applications, kinetic and potential energy changes are neglected. In the absence of those, exergy per unit mass for a system is[5],

$$b = (u - u_o) + P_0(v - v_0) - T_0(s - s_0) \quad (1)$$

where,

b = specific exergy

u, v, s = specific internal energy, specific volume and specific entropy of the system

u_0, v_0, s_0 = specific internal energy, specific volume and specific entropy of the dead state

P_0 and T_0 are the pressure and temperature of the dead state.

When the system is in equilibrium with the surroundings, the system is not able to produce any useful work. This state of the system is known as dead state [5]. Dead state is designated by affixing subscript '0' to the properties.

For flow periods, the flow exergy is given by,

$$b_f = (h - h_0) - T_0(s - s_0) \quad (2)$$

where,

b_f = flow exergy

h, s = specific enthalpy and specific entropy of the flow

h_0, s_0 = specific enthalpy and specific entropy of the dead state

For flows out of the system, the flowing matter is the cylinder contents, and for flows into the system the flowing matter must be specified [2].

The total exergy, B, can be evaluated with the above two expressions as,

$$B = mb \quad (3)$$

where, 'm' is the system mass and 'b' is the specific exergy.

As mentioned above, exergy can be destroyed by irreversible processes such as, heat transfer through a finite temperature difference, friction, combustion and mixing processes [5].

The destruction in exergy is given by [2],

$$B_{dest} = B_{start} - B_{end} + B_{in} - B_{out} + B_q - B_w \qquad (4)$$

where,

B_{dest} = exergy destruction due to irreversible processes

B_q = exergy transfer accompanying the heat transfer

B_w = exergy transfer due to work

Thus, using equations stated above, for a system the exergy balance is depicted in Figure 1[4].

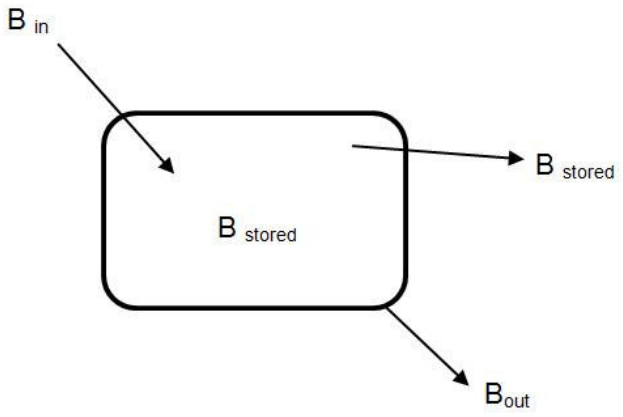

Fig. 1 Exergy balance for a system [4]

$$\sum B_{in} = \sum B_{out} + B_{stored} + B_{destroyed} \qquad (5)$$

Exergy associated with the work interactions is equal to the amount of useful work,

$$B_w = W \tag{6}$$

B_q is the available portion of heat transfer,

$$B_q = \int (1 - \frac{T_0}{T}) dQ \tag{7}$$

where, dQ =differential heat transfer, which is transferred at a system temperature T

B_{in} and B_{out} are the exergy values associated with flows[2],

$$B_q = \int (1 - \frac{T_0}{T}) dQ \tag{8}$$

The 'i' in the subscript denotes intake or exhaust process.

For complete exergy calculations, exergy associated with the fuel also needs to be determined. For the fuel, lower heating value (LHV) evaluated for a constant pressure process is used. The study uses isooctane as a fuel. For isooctane the relation is given by Heywood [1] as,

$$B_f = m_f (1.0286 \times LHV_f) \tag{9}$$

In brief the second law analysis facilitates the following:

a) Identifying processes involving destruction of energy
b) Quantifying the various losses

This analysis is particularly helpful for complex systems like turbocharged engines, turbo-compounding etc. Also, turbochargers have gained much popularity in high performance cars where they are used with spark-ignition engines to boost the power output. The next section reviews the basic principles of the way turbochargers function.

1.2 Turbocharging

In order to increase the specific power output of engines, engineers are opting for "downsizing" [6].Downsizing is a method in which reduction in engine size is achieved by coupling the engine with supercharging systems. The method has benefit of increased power due to supercharging systems without increasing size. The higher operating brake mean effective pressures (bmep) also means that turbocharged engines have lower pumping losses at low load [6].

In order to continually improve the performance of engines, engineers started using supercharging in various forms. Turbocharging is a specific method of supercharging. The hot exhaust gases from engine are used to drive the supercharging compressor [7].The exhaust gas-driven system was first employed by Büchi in the early twentieth century[7].In that system, compressor and turbine were housed in the same compact unit.

The actual working of turbochargers is explained in the following section. The hot exhaust gases which are at a higher pressure are expanded across a small turbine. The expanding gases drive the turbine and lose their energy. Thus, the gases exit at a lower temperature and pressure. As the turbine and compressor are coupled, the turbine drives the compressor at the same time. The compressed air from the compressor is then fed to the cylinders. The compression also elevates the temperature of the air. An intercooler is generally employed to cool this hot air and, in turn, to increase the air density. The higher density air enhances the combustion processes and leads to a higher power output. Figure 2 shows the layout of a common turbocharged engine.

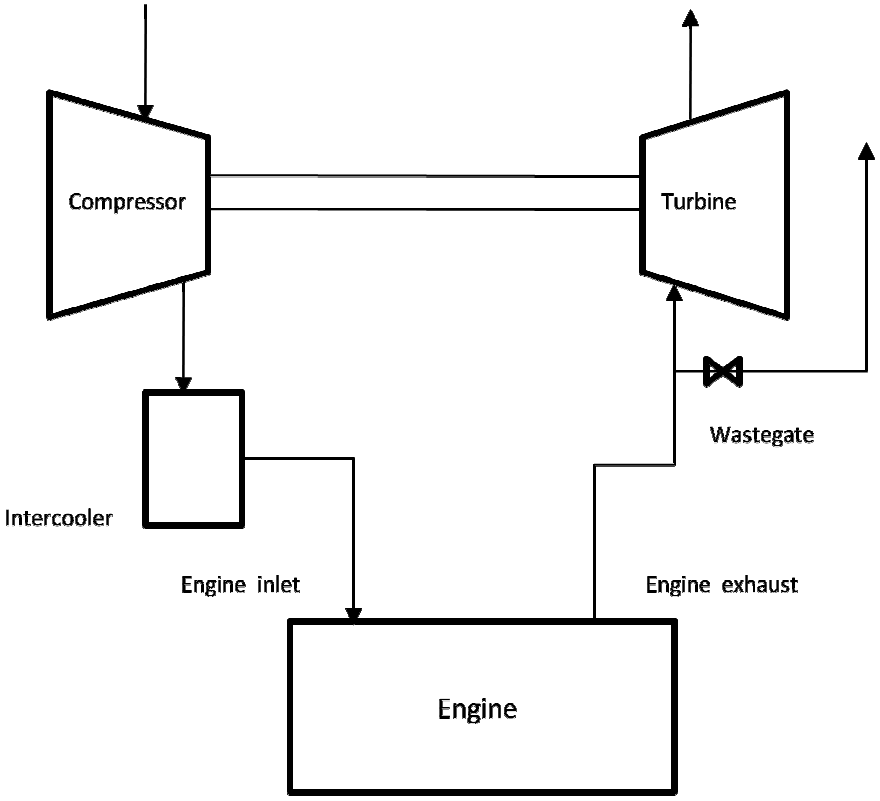

Fig. 2 Layout of a conventional turbocharged engine

This being said, there are still some problems in operation of turbochargers. One of them is the control of inlet or boost pressure. The turbochargers are designed for a specific boost pressure. Any pressure higher than the boost pressure could be detrimental to bothoc engine and the turbocharger itself. The solution for this is a simple valve called ‘waste gate’. The waste gate regulates the flow of exhaust gases to the turbine and operates mostly by the compressor outlet pressure. When the pressure exceeds boost pressure limit, the waste gate valve opens to bypass some of the gases to turbine. On the contrary, when pressure drops below certain value, the valve closes restricting flow of exhaust gases to turbine. An efficient design of waste gate can help optimize the torque curve within the knock limits [7].

2. LITERATURE REVIEW

Over the years, the second law analysis has improved continuously without fail. This technique has evolved from its beginnings to not only exploit various losses associated with processes but also suggest scope of improvement. The works on turbocharged engines extends from initial studies by Flynn *et al.*[8] to the recent study by Caton [2]. Over a dozen works including turbocharged engines have been summarized in following sections starting with the primary objective of second law analysis.

2.1 Overview of past works

Several studies have employed second law analysis to evaluate performance of both diesel and spark-ignition engines. In his recent study, Caton [2] has summarized second law investigations from the earliest project. The earliest research documented was in 1957 by Traupel[9]. More of such studies followed. Patterson and Wylen[10] determined exergy values for compression and expansion strokes for a spark-ignition engine cycle. The following studies focused largely on advanced diesel engines. Flynn *et al.*[8]analyzed turbocharged, intercooled diesel engines using second law analysis to quantify exergy values associated with heat transfer and exhaust. Diesel engines have been explored in great detail by many researchers since then. Spark-ignition engines and their advancements were not studied as extensively as diesel engines. Rakapoulos [4] included the transient operation of the spark-ignition engine in the second law analysis of using cycle simulation and validated the results using an experiment. Caton [11]developed a comprehensive thermodynamic cycle simulation for SI engines. Further, Caton [2, 11] found and quantified the exergy associated with heat transfer, combustion process and exhaust gases.

2.2 Studies on turbocharged spark-ignition engines

Numerous studies have focused on turbocharged spark-ignition engines. The studies have typically dealt with developing a simulation for turbocharged engine and exploring various effects of the addition of turbocharger on the spark-ignition engine. As, addition of turbocharger effects various aspects of engine like combustion, heat transfer, emissions, manifold pressures, etc., it is necessary to investigate these factors

in great detail. Works focusing on turbocharging aspects of spark-ignition engines are listed below.

Duchaussoy *et al.* [12] discussed the dilution effects on combustion of a turbocharged spark-ignition engine. As a part of the study, the authors [12] also presented comparisons between enrichment, exhaust gas recirculation (EGR) and lean burn as methods to control knock. The focus was on the thermodynamic aspect of knock control, which involved pressure and temperature control. Lean burn and EGR were employed at full load to analyze the combustion [12]. In the analysis, parameters like temperature and pressure-before-turbine were plotted as a function of equivalence ratio and EGR. The authors conclude that EGR and lean burn are both good strategies to avoid knock, but they also help in improving the indicated efficiency [12]. Lean burn and EGR give almost similar heat transfer benefit, but EGR reduces more fuel consumption.

Fillipi and Assanis[13] developed a computer simulation using 'filling and emptying technique' and used that for matching studies. In a 'filling and emptying' model, the intake and exhaust manifolds are treated as individual plenums and are sequentially filled and emptied with the flowing mass. A detailed discussion about this model is given in the following chapter. Fillipi and Assanis[13] examined a 1.1 liter, 4-cylinder prototype engine with the full load setting similar to a naturally aspirated engine. Results from the simulation model about the trends of parameters like boost pressure, friction mean effective pressure(fmep) and mechanical efficiency were in close accordance to actual data [13]. As a part of the study, the same model was used to predict the performance of a 1.4 liter engine. In addition, investigation was also done for the possible use of four valves per cylinder instead of two valves per cylinder. With the results of the study, Fillipi and Assanis [13] predicted that a four valves per cylinder engine gives about 4.3 percent to 15 percent increase in engine torque at medium and high loads. Also, the study analyzed the turbocharger performance at higher altitudes and established that turbocharger speeds were close to the allowed limit.

One of the problems associated with conventional turbocharging systems is that of matching the turbocharger with the engine [14]. At higher engine speeds, higher turbine entry pressures generate higher exhaust gas enthalpy [14]. A common solution to this excess turbine power is a wastegate valve. A unique solution to this problem could be 'variable geometry turbine' (VGT).

The study completed by Wang and Yang [14] puts forward a new concept called 'Turbocool turbocharging'. To exploit the benefits of VGT turbocharger completely, this method should be used in conjunction with it. The system employs an additional turbine–compressor unit to condition the intake air [14].The compressed air after the intercooler is directed to an added heat exchanger. Also, part of the air stream is passed to the turbocool turbine. The air stream expanding through the turbocool turbine undergoes expansion cooling and is then passed to the heat exchanger. Thus the actual air stream going to the cylinder attains further lower temperature. While the second air stream after the heat exchanger undergoes the compression heating process in the suction unit, this air stream exits to the ambient at a slightly higher temperature than the ambient [14]. The paper then compares the same concept with baseline turbocharged engines and naturally aspirated engines using computer simulation. According to the results of tests performed, the turbocool turbocharged engine can increase the power at 100 percent load by more than 20 percent relative to the baseline turbocharged spark-ignition engine and can be increased by almost 100 percent relative to the naturally aspirated spark-ignition engine. Wang and Yang [14] conclude that the new system proposed gives higher effective expansion ratio and improved engine performance relative to the turbocharged engine by utilizing the exhaust energy to condition the intake air.

In an attempt to study the effects of turbocharging on spark-ignition engines, Watts and Heywood[15] developed a simulation. The study compared the 5.7 liter, V-8, naturally aspirated engine with a downsized 3.8 liter, V-6, turbocharged engine but with similar maximum power. The primary factors analyzed were fuel consumption and NO_x emissions [15]. The idea of the study was to investigate the effects of reduced heat transfer due to turbocharging on engine performance. The simulation treated

engine cylinders as variable volume plenums and assumed a three-zone combustion model. NO_x formation was determined by the extended Zeldovich mechanism. A simulation study for part-load operation of turbochargers was also performed [15]. This validated the model's ability to predict the engines' performance over varying loads at the same speed. For validation, the study describes the brake mean effective pressure and brake specific fuel consumption as a function of load for part-load operations, which is largely in agreement with actual data [15].

Watts and Heywood [15] further compared the two engines for brake specific fuel consumption variation. The study summarizes that same power turbocharged engines always have lower fuel consumption than naturally aspirated engines. The study also stated that a 3.8 liter, turbocharged engine is more efficient than a 5.7 liter, naturally aspirated at the same power level as it has higher mechanical efficiency.

Li and Karim [16] discussed the various approaches to suppress the onset of knock for natural gas-powered turbocharged spark-ignition engines. They [16] suggested a range of strategies to increase the knock limited boost pressure ratio for turbocharged engines. One of the techniques could be through increasing the after cooler effectiveness to reduce the knock, but this limits the boost pressure ratio. The study summarized that EGR cooler effectiveness above 0.62 is helpful in reducing the onset of knock [16].

2.3 Second law studies

Use of the second law to assess engine performance has been in practice for several decades now [2]. A comprehensive review of all such instances is available in the work by Caton[2]. The paper summarizes all different approaches dating back to 1957 to the more recent ones of 2000. Rakapoulos and Giakaoumis[3] continued on the same study but with an emphasis on in-cylinder processes and different forms of exergy. The study[3] also considers the engine along with its subsystems like turbochargers for the exergy analysis. It is evident from both the papers that much work has been done for the compression-ignition engine and comparatively less information is available for the spark-ignition engine [2, 3]. In the case of spark-ignition engines,

almost all of the work has been focused on naturally aspirated engines and no data is available in regards to turbine and compressor irreversibilities [3]. For diesel engines employing turbochargers, a lot of work has been done as turbocharged diesel engines have become a norm.

One of the earliest works in this field was done by Flynn *et al.*[8]. They studied the application of the second law to a turbocharged diesel engine. Compressor, aftercooler and turbine were treated as separate subsystems. Flynn *et al.* also quantified the exergy terms associated with the processes as a fraction of fuel exergy for all the subsystems [8]. Primus *et al.*[17] published a paper supporting the methodology used by Flynn *et al.*[8]. The study focused more on the comparison of naturally aspirated and turbocharged diesel engines. Moreover, they also investigated benefits of turobocompunding, charge air cooling and insulating techniques. Exergy balance for all the different engine configurations were quantified as a percentage of fuel exergy. In the case of turbochargers, it was established that lean mixture combustion of turbocharged engine leads to higher combustion exergy losses compared to naturally aspirated engines. This phenomenon occurs due to increased mixing and lower bulk gas temperatures. Mixtures close to stoichiometric were shown to reduce exergy loss due to combustion. Based on this important finding, the authors proposed that charge air cooling reduces exergy destruction associated with the heat transfer.

A different approach for the turbocharged diesel engines has been presented by Bozza *et al.* [18]. This study suggests that mechanical input is increased due to an increase in fuel and air rates, but it cannot be linked to turbocharging. In addition, the study states that turbocharging may lead to further losses due to increased mass and energy rates through the manifolds and also due to increased flow through turbines and compressors [18]. But the study also admits that turbocharging indeed enhances the combustion process when the boost pressure is increased.

As proposed by Bozza *et al.*[18], the objective of the second law analysis should be investigating the methods to reduce the losses in exergy and exploit other forms of

available energy other than piston work. Thus, principal focus of studies listed above was on examining various irreversibilities associated with engine processes and subsystems. All the cases reviewed above were helpful in understanding the nature of the different studies conducted for turbocharged engines as a part of the second law analysis. Though most of the work described above has been performed for compression-ignition engines, they give a fair amount of basic knowledge about the behavior of different processes in an engine and the efficiencies associated with it.

To summarize, the second law analyses have been a focus of most of the engine research in the recent years. Principally, diesel engines were the area of interest for most of the works. Compression-ignition engines even in their complex forms like IDI engines and turbocharged engines have been investigated for exergy balance and in-cylinder operations[3]. On the contrary, all the spark-ignition studies have dealt with only naturally aspirated engines for exergy balances and in-cylinder operations.

3. MOTIVATION AND OBJECTIVES

From the literature acknowledged above, it is evident that the majority of research involving second law analyses has been done on diesel engines and their components. Comparatively, spark-ignition engines and their components like turbochargers have not been studied as much with the second law analyses.

To put it briefly,

a) The lack of literature on the second law analysis of turbocharged spark-ignition engines was one of the primary motivations behind this study.
b) Also this study draws insight from the project performed by Watts and Heywood[15].The same two engines 5.7 liter, V-8 and 3.8 liter, V-6 compared in the said study[15] were analyzed using the second law.
c) As turbocharged spark-ignition engines are becoming popular in conventional and high performance automobiles [13], investigations using second law analyses will give a good insight into the turbocharged spark-ignition engines and may lead to further improvements in performance.

3.1 Objectives

The principal objective of the study was to investigate for a spark ignition engine, the components of a turbocharger for irreversibilities, using a second law analysis. Also comparison of the naturally aspirated engine with the turbocharged engine was one of the key goals of this study. The following is the brief scope the current study.

3.2 Scope of this study

The analytical approach selected has significant advantages over the experimental approach. Engine models offer unique ways to analyze critical features of a process [1]. Many works in this field have chosen simulation over experiments for its evident advantages. There has been a considerable amount of research done on the diesel and spark-ignition engines with the help of simulation. As a result, there is an existing framework which can be employed and further modified. The proposal to investigate the turbocharged spark-ignition engine was largely based on this fact. Also, for a

deeper insight into the processes of a subsystem like turbocharger for a spark-ignition engine, the second law analysis was needed. Thus for the current study, this existing and widely known medium of simulation cycles was selected. The strategy for this project was to study the current research on second law analysis of spark-ignition engines. Based on the previous studies, a model was to be developed. The works in this field will serve as a guide to the current study.

Recent studies by Caton [11] and Shyani and Caton [19] employed simulation for the second law analysis of the spark-ignition engine. The current study uses a similar simulation with an added feature to analyze the turbocharger. The following section describes a few studies in this field and their relevance to the current project and the primary objectives of this work.

Watts and Heywood [15] compared the turbocharged and naturally aspirated spark-ignition engine for part load operations. Similar engines were compared at part-load operations in current study using the second law analysis. Watts and Heywood [15] made an observation that the downsized turbocharged engine was more efficient than the naturally aspirated engine. The reason for the improved efficiency was credited to the higher mechanical efficiency of the turbocharged engine [15]. One of the primary objectives of the current study was to validate this claim using the second law analysis.

On the contrary, Bozza *et al.*[18] predicted that turbocharging for a diesel engine may not improve mechanical efficiency, but it indeed enhances the combustion process. Thus, it becomes essential to analyze and evaluate the effects of turbocharging on an engine to give greater insights into engine operations. With the help of the second law, the in-cylinder processes can be explored for exergy values. Exergy would be the ideal parameter to measure the performance of a process, as it will give an indication of irreversibility or exergy destroyed in a process. Less irreversibility implies losses will be lower and the process will be efficient. As a result, the current study is focused on finding the exergy balance for all the processes including those in the added turbocharger unit. With this background, a simulation was developed to conduct this

study. A comprehensive discussion of the simulation model and its nuances are given in the subsequent section.

4. SIMULATION DESCRIPTION

The present study employs the thermodynamic cycle simulation of spark-ignition engines, as used by previous studies. In the present study, however, a new feature was added. The new feature included the ability to examine turbocharging of real spark-ignition engines and included the use of the first and second laws of thermodynamics.

4.1 Previous studies

Previous studies employed the simulation to investigate the spark-ignition engine with the help of the second law analysis (e.g.[19]). The simulation is a complete representation of all thermodynamic processes for the intake, compression, combustion and exhaust events. The simulation uses a three-zone combustion model. A detailed explanation of the simulation for conventional spark-ignition engine is given in the work by Caton[11]. The cylinder heat transfer is adopted from the correlation by Woschni[20], and the combustion process governs Wiebe relations for mass fractions burned.

Some of the input parameters to the simulation are engine geometry, engine speed(N), equivalence ratio(ϕ), combustion duration(θ_b), start of combustion timing(θ), Intake manifold pressure(P_{in}), temperature after intercooler before intake(T_{ind}), compression ratio(r) and exhaust gas recirculated(EGR). The simulation then calculates various output parameters. Some of the output parameters are indicated power, brake power, brake mean effective pressure and brake specific fuel consumption at the selected operating point. The simulation also predicts unburned and burned mixture temperatures as a function of crank angle and mass flow rate through the engine and cylinder pressures. The simulation also performs exergy calculations for the complete cycle by quantifying exergy values associated with all the processes.

4.2 Present study

The present study is derived from the same simulation as mentioned above but with added turbocharger features. Consequently, it shares many common input

parameters and a few additional ones related to the turbocharger. For the turbocharger, the input parameters are efficiencies of the compressor and the turbine (η_{comp} & η_{turbo}) and the intercooler effectiveness (ε). The simulation also has the ability to switch off the turbocharger operation to perform as a naturally aspirated engine. In addition to the output parameters of the previous simulation model, the present model also calculates the temperatures at the exit of the turbocharger and the compressor. The amount of exhaust bypassed through the wastegate is also calculated for the turbocharger. Exergy calculations are done now for the engine and turbocharger combined.

The following section gives details about the simulation, the assumptions, and definitions associated with it, followed by the description of engines and operating conditions.

4.3 Model description

This section illustrates the significant features of the present thermodynamic model which helps in better understanding of the analysis. The prominent features are basic assumptions, definitions and various models like the combustion model and the 'filling and emptying' model.

4.3.1 Basic assumptions

The assumptions for the simulation remain the same as the previous study with additional assumptions made for the turbocharger [19]:

1. Contents of the cylinder constitute the thermodynamic system.
2. The engine is in steady state such that the thermodynamic state at the beginning and at the end of the cycle is identical.
3. The cylinder contents are spatially homogenous and occupy one zone for the compression, expansion and exhaust process.
4. The two zone model is used for the intake process. One zone corresponds to fresh charge and other zone consists of residual gases.

5. A three zone model was employed for the combustion process. The three zones are the adiabatic core burned zone, unburned zone and burned zone at the boundary layer.
6. The thermodynamic properties vary only with time (crank angle) and are spatially uniform in each zone.
7. Quasi-steady, one dimensional flow equations are used to determine the air flow rates and intake and exhaust manifolds are treated as plenums containing gases at constant temperature and pressure.
8. The fuel is completely vaporized and mixed with the incoming air.
9. The blow-by is assumed to be zero.
10. Air fuel mixture was assumed to be stoichiometric (ϕ=1).
11. Combustion duration was assumed to be at 60°CA.
12. Start of combustion was determined for maximum brake torque (MBT).
13. For most of the cases, the isentropic efficiencies of the turbocharger and the compressor were assumed to be constant at 65%; the intercooler effectiveness was assumed to be constant at 60%.

4.3.2 Definitions

a) Brake Mean Effective Pressure(bmep)

Mean effective pressure is obtained by dividing the work per cycle by the volume displaced per cycle [1] . In other words, brake mean effective pressure is the mean pressure which when applied uniformly to the cylinders at each power stroke will produce the same brake power.

$$mep = \frac{P \times n_r}{V_d \times N} \qquad (10)$$

P=power

n_r=no of crank revolutions for each power stroke

V_d= volume displaced

N= engine speed (rpm)

$$bmep = \frac{P_b \times n_r}{V_d \times N} \tag{11}$$

b) Brake specific fuel consumption (bsfc)

Specific fuel consumption is the fuel flow rate per unit power output [1]. It measures how efficiently engine uses the supplied fuel. Brake specific fuel consumption compares fuel flow rate with brake power.

$$bsfc = \frac{m_f}{P_b} \tag{12}$$

c) Start of combustion (θ_0)

The crank angle corresponding to start of combustion is specified as an input (θ_0). Ignition timing is optimized for maximum power. For all the calculations, the ignition timing was arranged at MBT (maximum brake torque) [1].

d) Combustion duration (θ_b)

Combustion duration is also one of the inputs and generally assumes a constant value for all calculations. Figure 3 illustrates the start of combustion and combustion duration. Combustion duration is the crank angle interval from start of combustion to the angle where mass fraction burned reaches the value of 1.

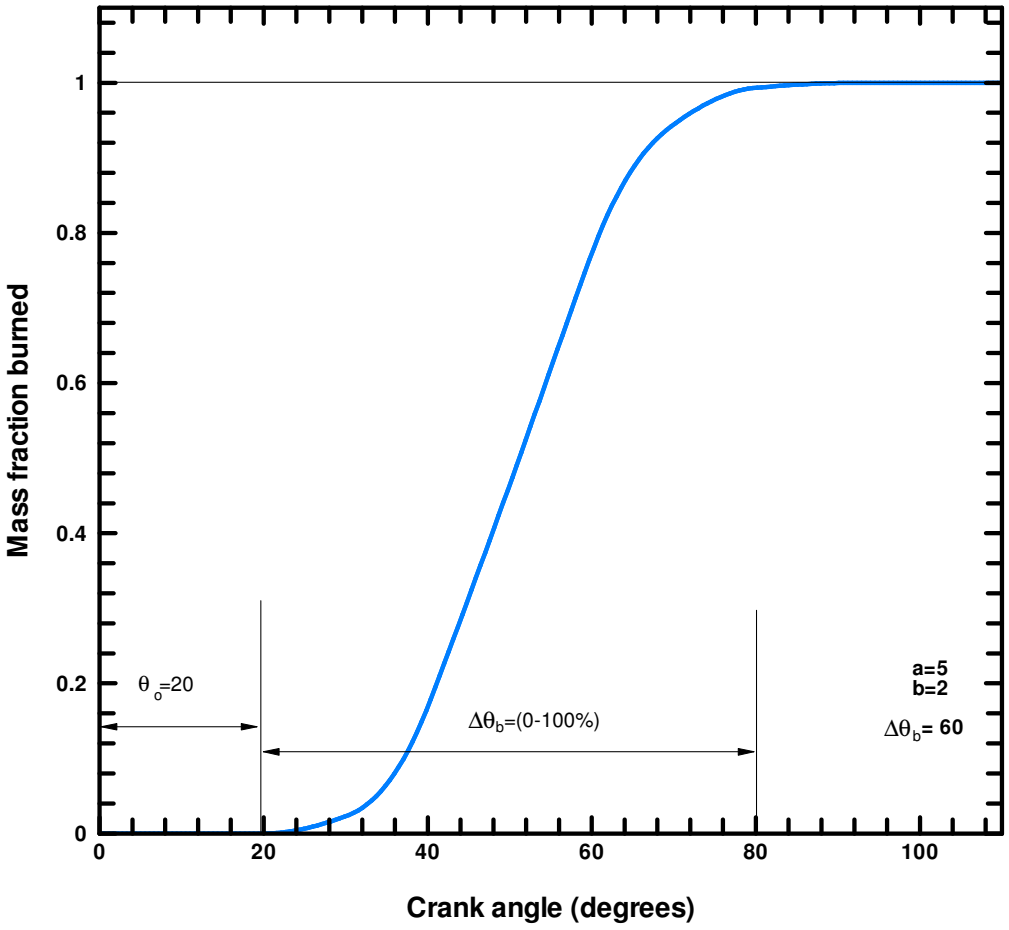

Fig. 3 Schematic of mass fraction burned profile,θ_0 is the start of combustion, $\Delta\theta_b$is the duration of combustion

4.3.3 Combustion model

The combustion model employed is a three zone combustion model. Figure 4 depicts the three zones. The model starts with a burned and an unburned zone first. Later the burned zone is assumed to extend into an adiabatic zone and a boundary layer. At the start of the combustion process, the boundary layer has zero mass and the adiabatic zone is the burned mass.

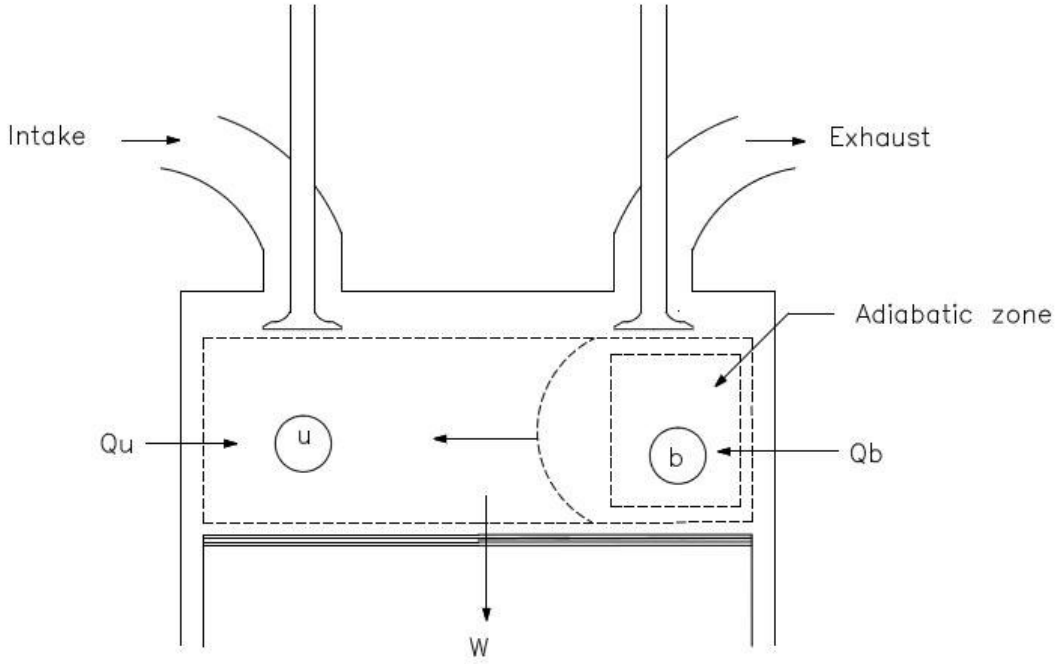

Fig. 4 Schematic of the engine with control system and depicting the different combustion zones, 'u' is the unburned zone and 'b' represents burned zone[11]

Adiabatic zone temperature is assumed to be a linear function of wall temperature. The average boundary layer temperature can be expressed as,

$$T_{bl} = \frac{(T_a - T_{wall})}{\ln \frac{T_a}{T_{wall}}} \qquad (13)$$

where,

T_a=adiabatic zone temperature

T_{wall}=wall temperature

The mass fraction of the air-fuel mixture burned in the cylinder at any crank angle is specified by the Wiebe function.

$$x = 1 - e^{-a\left(\frac{\theta-\theta_0}{\Delta\theta_b}\right)^{m+1}} \quad (14)$$

x= fraction of the mass burned in the cylinder

a= efficiency parameter

m= form factor

θ= crank angle

θ_0= start of combustion

$\Delta\theta_b$= combustion duration

4.3.4 Filling and emptying model

The intake and exhaust systems govern the air flow into the cylinders. As air flow has a great influence on combustion and thus the power produced, the design of intake and exhaust systems is of prime concern. The current study applied the 'filling and emptying' model to design intake and exhaust systems.

In 'filling and emptying' models, each manifold or cylinder is treated as a control volume and is successively filled and emptied as mass passes through the engine [7]. The basic energy and mass conservation equations are applied to each control volume. Then, energy and continuity equations are solved for each one. With the help of these equations, the model can define the state of the gas for each control volume at the start. The calculations are done for each crank angle. Numerical methods like Runge-Kutta are used to calculate estimates of properties like temperature, pressure and mass at each time interval[7]. Thus, the thermodynamic state is defined at each step, enabling the calculation of work output per cycle [7] .

Filling and emptying models have also been used successfully for turbocharger matching. The turbocharger can either be simulated by a nozzle in the exhaust with boost conditions specified independently or by using complete characteristics of the turbocharger[7].Filling and emptying programs are frequently used for intial turbocharger matching studies for new and updated engines [7].The accuracy with

which the model can predict pressure pulsations in manifolds is limited by the size of manifolds [7]. The model is suited for small manifolds as a predictive tool [1].

4.3.5 Extension of model- addition of turbocharger

As mentioned above, the current study included a feature to use the turbocharger for a spark ignition engine. The addition of the turbocharger required the selection of appropriate engine operating conditions. The new components added were the compressor, turbine and intercooler. The following describes the new capabilities of the model.

Figure 5 is a schematic of the new system. The work of the turbine is exactly equal to the required work of the compressor. For most of the conditions, only a portion of the exhaust is necessary for the turbine work. The excess exhaust is 'by-passed' directly to system discharge. New exergy destruction terms are introduced due to compressor and turbine irreversibilities. A detailed section predicts energy values associated with processes like heat transfer, exhaust and intercooler along with the brake energy, all values per cylinder. Exergy values are also calculated for the above mentioned processes together with new terms like exergy destruction at the compressor and the turbine, destruction due to flow past valves. The simulation also performs exergy balance for all the processes- combustion, intake, exhaust, compression as well as at the intake and exhaust valves.

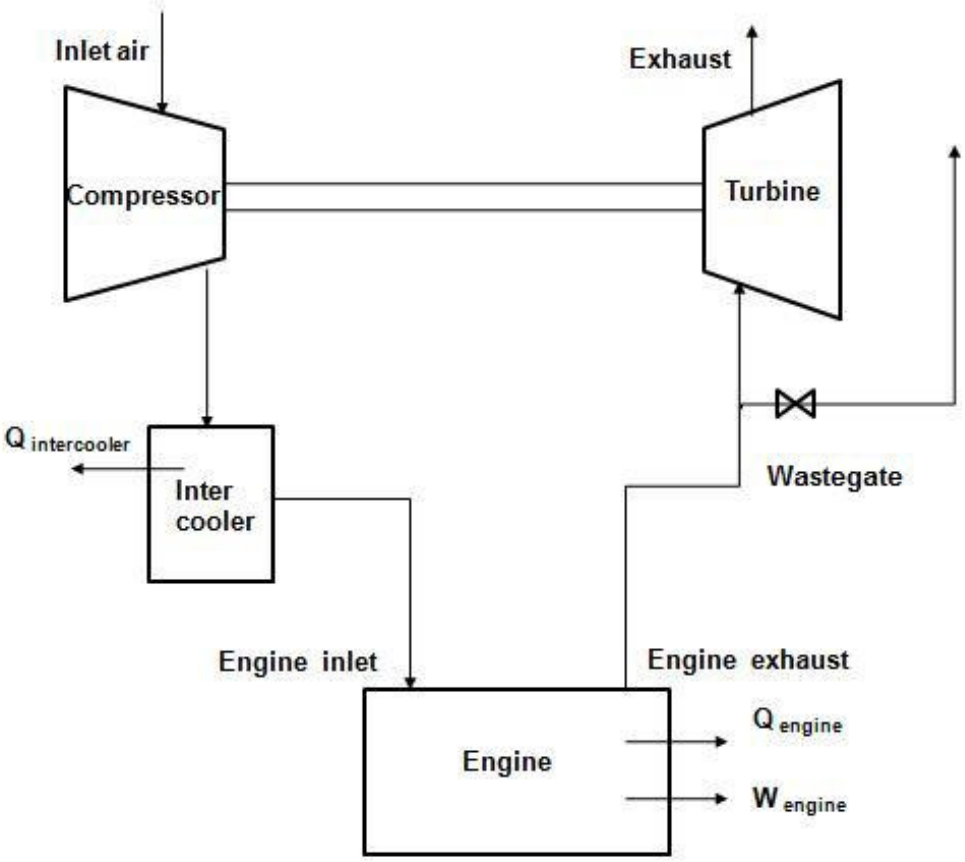

Fig. 5 Schematic of engine with turbocharger components

For validation of the simulation over the entire speed and load range, few input parameters were provided at every operating point. Inlet and exhaust manifold pressures were one of the parameters provided at a given point. Figure 6 shows these pressures as a function of engine speed. The inlet manifold pressure increases from 1000 rpm to 2500 rpm and then remains constant at about 168 kPa. On the other hand, the exhaust pressure continually increases due to an increase in mass flow as engine speed increases.

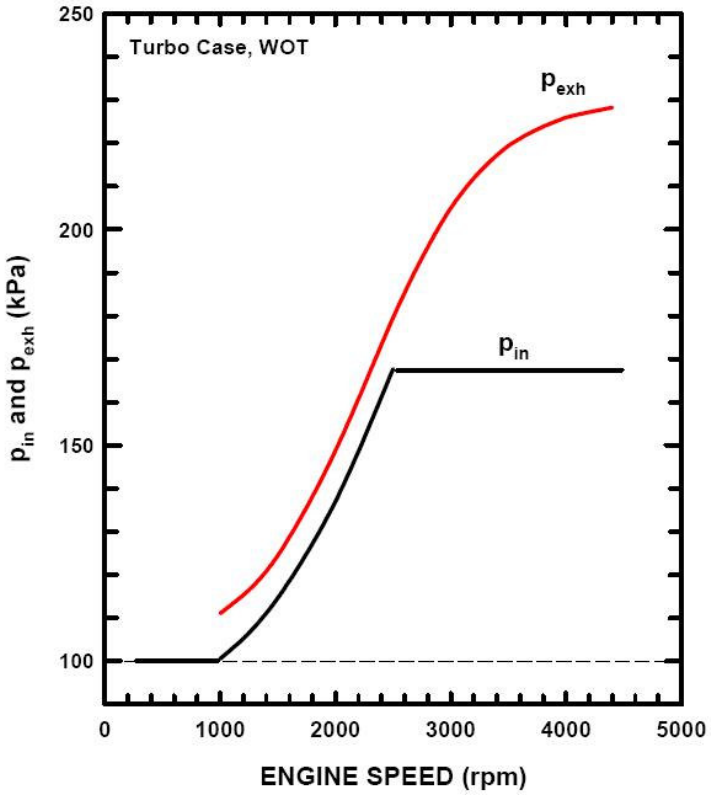

Fig. 6 Inlet and exhaust manifold pressures as functions of engine speed for the WOT conditions

The base case was selected at an engine speed of 2000 rpm. Details about the significance of selecting the appropriate operating point for the base case are discussed in the next chapter. The other operating parameters like equivalence ratio and combustion duration were assumed at a constant value mentioned above, to avoid ambiguity as other parameters are varied.

5. RESULTS AND DISCUSSION

Results obtained from this study are illustrated in this section. It is essential to know the limitations of the study in advance. Engine details and specifications follow the limitations section. The results are then described in the final section.

5.1 Limitations of the study

Cyclic variations in the combustion process were not taken into account in this simulation study[19]. Cyclic variations are caused due to

- variation in mixture motion within the cylinder at the time of spark cycle by cycle,
- variation in the amounts of air and fuel fed to the cylinder each cycle,
- changes in mixing of fresh charge and residual gases within the cylinder each cycle, particularly in the vicinity of the spark plug.

Due to the differences in the same phenomenon, variations between cylinders are also caused. Capturing these mentioned aspects in the simulation is very difficult. Thus for convenience these variations were neglected.

Also, blow-by was assumed to be zero for the present study. The engine combustion chamber is connected to small volumes called crevices. During actual operation of the engine, due to pressure changes, some of the fuel, air and moisture are forced past the piston rings to the crankcase. This phenomenon can be attributable to wearing of parts and soot, deposits, etc. Also, in the present study the possibility of spark or auto ignition was not considered.

The simulation was developed only for steady state operation of the engine and does not take into account any transient operation. Moreover, the performance maps were not used to define the compressor and the turbine.

5.2 Engine details and specifications

The engine selected for the study is an automotive, turbocharged 3.8 liter, V-6 engine. The engine selected for the comparison is an automotive, naturally aspirated, 5.7 liter,

V-8 engine. Engines selected are the representatives of their class of application. Specifications of turbocharged engine are listed in Table 1.

Table 1 Specifications of the turbocharged engine

Item	Value
Number of cylinders	6
Bore (mm)	96.5
Stroke (mm)	86.4
Crank Rad/Con Rod	0.305
Compression Ratio	8.0:1
Inlet Valves:	
Diameter (mm)	41.3
Max Lift (mm)	8.75
Opens (°CA aTDC)	344
Closes (°CA aTDC)	-124
Exhaust Valves:	
Diameter (mm)	36.2
Max Lift (mm)	8.75
Opens (°CA aTDC)	110
Closes (°CA aTDC)	396

5.3 Base operating conditions

In practice, the spark-ignition engines envelop a wide range of operating conditions. But, it is helpful to select a reference point at which the engine speed and load are held constant- called the base operating point. It is also equally important that the reference point selected should be representative of the typical operating range of the engine.

As the turbocharger affects engine performance over about half of the engine load range [15], an engine speed of 2000 rpm was selected for the current study. The other input parameters at base case were inlet pressure of 137 kPa, outlet pressure at 148.8 kPa, equivalence ratio of 1.0,spark timing at MBT, compression ratio 8:1 and

combustion duration of 60°.Table 2 lists various fuel input parameters and engine operating conditions for base case at Wide open throttle (WOT).

Table 2 Engine and fuel input parameters, base case: 2000 RPM, WOT, MBT timing

Item	Value used	How Obtained
Engine Speed (rpm)	2000	Input
Displaced Volume (dm^3)	3.791	Computed
AF_{stoich}	15.13	For Isooctane
Fuel LHV (kJ/kg)	44,400	For Isooctane
Equivalence Ratio	1.0	Input
Frictional mep (kPa)	88.2	Algorithm
Inlet Pressure (kPa)	137.0	Input
Engine Exit Pressure - Turbine Inlet Pressure (kPa)	148.8	Input
Turbine Exit Pressure – Exhaust System Pressure (kPa)	105.0	Input
Start of Combustion (°bTDC)	24.0	Determined for MBT
Combustion Duration (°CA)	60	Input
Cylinder Wall Temp (K)	450	Input
Compressor Inlet (ambient) Temperature and Pressure	300 K 100 kPa	Input
Compressor Isentropic Efficiency	65.0%	Input
Turbine Isentropic Efficiency	65.0%	Input
Intercooler Isentropic Efficiency	60.0%	Input
Coolant Inlet Temperature to Intercooler (K)	310	Input

As mentioned in the section 4.3.2, the start of combustion was determined for MBT. Figure 7 illustrates this concept. From the figure, it can be seen that the maximum is fairly flat for the curve. Thus, ignition timing is usually arranged to occur on the late side of the maximum [21]. There are many ways to define MBT timing. Generally, it corresponds to the timing when the first fall in the peak torque is observed [21].

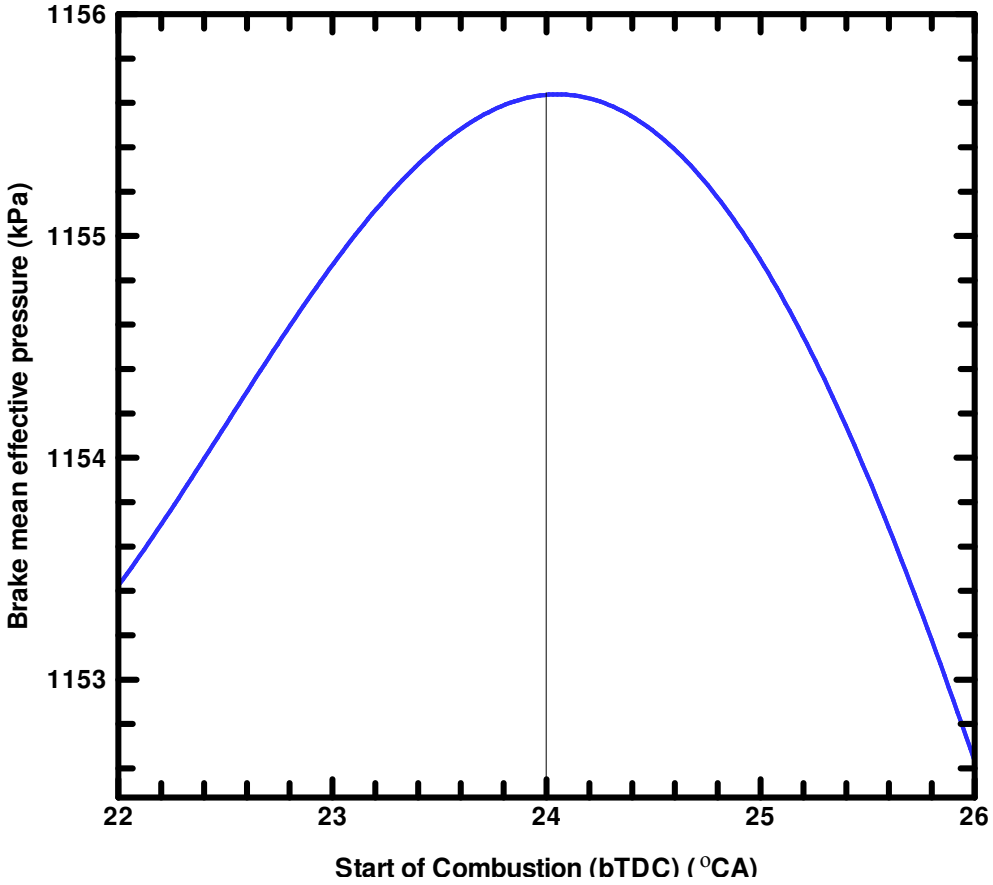

Fig. 7 The effect of ignition timing on output of spark-ignition engine

5.4 Results of the study

The current study was primarily divided into two parts, one focused on turbocharged engine alone and the other concentrated on comparative studies between the turbocharged and the naturally aspirated engine. Thus, results from this study are categorized in two sections accordingly.

5.4.1 Results from the turbocharged engine study

a) Operating at base case (2000 rpm) wide-open-throttle (WOT)

Table 3 lists the percentage of fuel energy and fuel exergy values associated with various items. The fuel energy is divided between indicated work, engine heat

transfer, exhaust gas, intercooler heat transfer and unused fuel. The work associated with the turbine and the compressor is equal for the whole system, and since the work is in balance, it is not listed.

Table 3 Energy and exergy balances for the base case, 2000 rpm, WOT, MBT timing

Item	Energy (%)	Exergy (%)
Indicated Work	33.76	34.70
Heat transfer	20.99	16.79
Net flow out	41.06	23.10
Intercooler	0.95	0.11
Dest Combustion	n/a	20.54
Dest Compressor	n/a	0.46
Dest Turbine	n/a	0.24
Dest Inlet	n/a	1.44
DestExh	n/a	1.94
Unused fuel	0.68	0.67
Total	100	99.99

Table 3 leads to some important conclusions. On comparing the set of values, it is clear that the exergy percentage associated with the heat transfer (16.79%) is slightly less than the energy percentage associated with the heat transfer (20.99%), since not all heat transferred is able to produce useful work. Correspondingly, the exergy percentage associated with the exhaust flow (23.10%) is less than the energy percentage associated with the exhaust flow (41.06%). The major new items introduced due to turbocharging are the exergy destruction associated with the turbine, the compressor and the exhaust flow.

It should be noted that for the second law analysis, the desired output is brake power and increases in this quantity will represent improved performance. All other terms

signify losses or undesirable transfers from the system and decreasing these terms will lead to an enhanced performance[1].The most important exergy destruction term remains the combustion process. For the base case, the exergy destruction due to combustion is about 20.54 per cent of the fuel exergy. The other exergy destruction terms in the order of their decreasing importance are exhaust flow (1.94%), inlet flow (1.44%), compressor (.46%) and turbine (0.24%). Thus, use of turbocharging does not add significantly to the overall irreversibilities.

As mentioned in Section 4.2, for every operating point a set of input parameters necessary for operation, were provided. Table 4 gives the operating conditions as a function of engine speed. The input parameters for this computation were engine speed, equivalence ratio, combustion duration, spark timing (MBT), inlet and outlet pressures. The values of bmep and bsfc were computed at each speed using the simulation.

Table 4 Bmep and bsfc as a function of engine speed for base case,WOT

Speed (rpm)	**ϕ**	**θ_b (^oCA)**	**θ_o (^oCA bTDC) (MBT)**	**p_{in} (kPa)**	**$p_{exh\ manifold}$ (kPa)**	**bmep (kPa)**	**bsfc (g/kW-h)**
1000	1.0	60	20	100.0	111.1	638.9	273.1
1200	1.0	60	20	105.2	115.3	754.5	262.7
1500	1.0	60	21	114.7	124.5	907.6	253
2000	1.0	60	24	137.0	148.8	1155.9	244
2500	1.0	60	24	167.7	179.6	1467.1	237.8
3000	1.0	60	24.5	167.7	205.0	1350.2	242.5
3500	1.0	60	25	167.7	219.4	1319.5	245.7
4000	1.0	60	25.5	167.7	226.0	1313.3	248.1
4400	1.0	60	25.5	167.7	228.3	1310	250

The wide-open-throttle characteristics listed above for the turbocharged engine are depicted graphically, in Figure 8. The bmep values increased with an increase in engine speed till the engine speed of 2500 rpm. After the engine speed of 2500 rpm, the wastegate system gets activated and the bmep values achieve a steady value. This can be attributed to the increased pressure in the cylinder due to turbocharging. Bsfc values also exhibited similar trend. The values of bsfc decreased continuously but after the engine speed of 2500 rpm, bsfc values attained a steady value. As, the bsfc is the reciprocal of brake thermal efficiency, brake thermal efficiency values if plotted will display the reverse trend. The brake thermal efficiency values will exhibit an increase for approximately half of the speed range and then will attain a steady value.

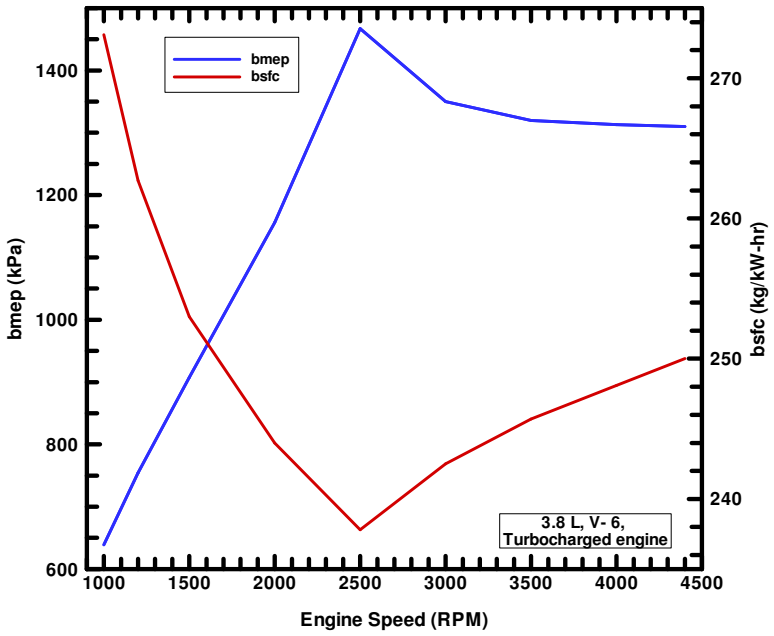

Fig. 8 Operating characteristics of the turbocharged engine at base case- 2000 rpm, WOT

b) Exergy destruction for turbocharger components

Next, the effects of a few input parameters on exergy destruction terms in the turbine and the compressor were examined. The above mentioned terms as a percentage of fuel exergy were varied as a function of isentropic efficiency for the base case. Table 5

gives the values of exergy destruction of components as a function of component isothermal efficiency.

Table 5 Exergy destruction in turbine and compressor as a function of isentropic efficiency for the base case, 2000 RPM, MBT timing

Turbine/Compressor efficiency	Exergy destruction (%of Fuel Exergy)	
(%)	Compressor	Turbine
50	0.84	0.56
60	0.57	0.32
70	0.37	0.18
80	0.22	0.09
90	0.1	0.04

Figure 9 presents the trends from this study. Dotted line indicates the data for the compressor and solid line shows the exergy destruction values for the turbine. For both the components, the exergy destruction decreased with increasing efficiency of components. For the current conditions, exergy destruction was low. Also, it is important to note that the exergy destruction for turbine was lower than the compressor as only some portion of the flow moves through the turbine and the rest is bypassed.

Similarly, exergy destruction terms due to the turbine and the compressor, expressed as a percentage of fuel exergy above, were plotted as a function of engine speed for WOT conditions.

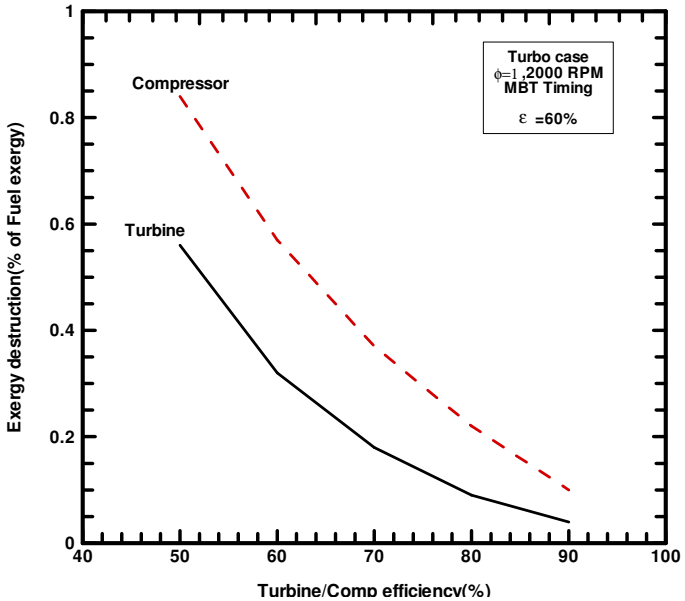

Fig. 9 Exergy destruction due to the compressor and the turbine, as a function of isentropic component efficiencies for the base case, 2000 rpm

Table 6 shows the values for this study. The exergy destruction terms (% of fuel exergy) associated with the compressor and turbine are listed as a function of the engine speed.

Table 6 Exergy destruction due to the turbine and the compressor as a function of engine speed, WOT

Speed (RPM)	Exergy destruction (%of Fuel Exergy)	
	Compressor	Turbine
1000	0	0
1200	0.08	0.04
1500	0.21	0.1
2000	0.46	0.24
2500	0.74	0.4
3000	0.74	0.41
3500	0.75	0.27
4000	0.75	0.27
4400	0.75	0.27

Figure 10 displays the results from Table 6. Again the exergy destruction values for the compressor are indicated by the dotted line and solid lines represent exergy destruction values for the turbine. The exergy destruction values are plotted as a function of the engine speed. The exergy destruction terms increased with an increase in the engine speed for both the components. At about 2500 rpm, the values reach their peak. After that, the boost control system or the wastegate comes into effect. Thus, the values did not increase much with the increasing engine speed afterwards. Again, the exergy destruction term due to the turbine was considerably lower than that due to the compressor, for the same reason mentioned above.

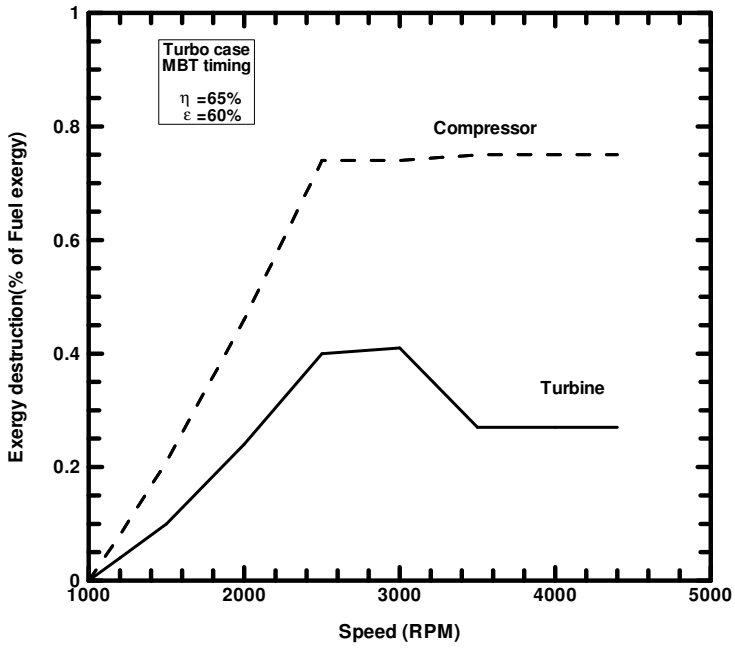

Fig. 10 Exergy destruction due to the turbine and the compressor as a function of the engine speed, WOT conditions

c) Study to examine the effect of turbocharging on combustion irreversibility

In an attempt to determine the behavior of combustion irreversibility over the entire speed range an additional computation was performed. Table 7 lists the values from

this study. The schedule from base case (Table 4) was employed and exergy destruction due to combustion was computed at each engine speed.

Table 7 Variation of combustion irreversibility with the engine speed, WOT

Speed (rpm)	ϕ	θ_b (^oCA)	θ_o (^oCA bTDC) (MBT)	p_{in} (kPa)	$p_{exh\ manifold}$ (kPa)	bmep (kPa)	bsfc (g/kW-h)	Destruction of exergy due to combustion (%)
1000	1.0	60	20	100.0	111.1	638.9	273.1	21.22
1200	1.0	60	20	105.2	115.3	754.5	262.7	21.03
1500	1.0	60	21	114.7	124.5	907.6	253	20.83
2000	1.0	60	24	137.0	148.8	1155.9	244	20.39
2500	1.0	60	24	167.7	179.6	1467.1	237.8	20.29
3000	1.0	60	24.5	167.7	205.0	1350.2	242.5	20.22
3500	1.0	60	25	167.7	219.4	1319.5	245.7	20.19
4000	1.0	60	25.5	167.7	226.0	1313.3	248.1	20.14
4400	1.0	60	25.5	167.7	228.3	1310	250	20.12

Figure 11 displays the graph of combustion irreversibility as function of the engine speed. Combustion irreversibility values decreased sharply till the engine speed of 2000 rpm. Thereafter, the values displayed steady drop but overall, the combustion irreversibility values decreased continuously over the entire speed range. This decrease can be attributed to the higher maximum temperatures in the engine cylinders. The maximum temperature inside the cylinders increases due to the turbocharging and combustion irreversibility decreases at higher maximum temperatures.

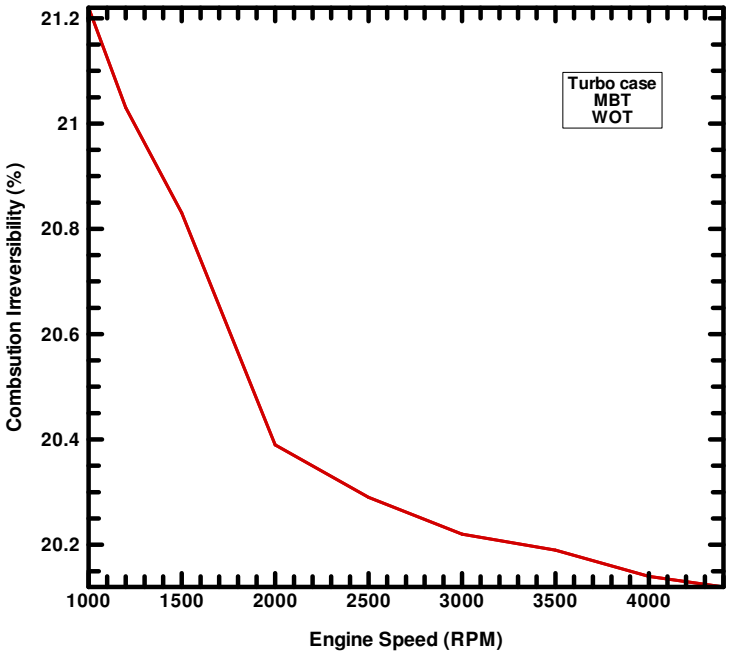

Fig. 11 Combustion irreversibility as a function of the engine speed, WOT

Similarly, a study was performed at part loads to investigate the effect of turbocharging on combustion irreversibility. For part loads, a schedule similar to the base case was provided as an input. Table 8 gives the operating conditions for part load operation. After employing the schedule from Table 8, exergy destruction due to combustion or combustion irreversibility was calculated with the help of the simulation.Table 9 displays the values from this study.

Table 8 Operating parameters for part load, 2000 rpm

Speed (rpm)	ϕ	θ_b (^oCA)	p_{in} (kPa)	$p_{exh\ manifold}$ (kPa)
2000 s(throttled)	1.0	60	54.0	103.4
2000 (throttled)	1.0	60	75.4	105.0
2000 (throttled)	1.0	60	94.4	113.9
2000 (Turbo)	1.0	60	108.3	123.0
2000 (Turbo)	1.0	60	123.9	136.1
2000 (Turbo-Full load)	1.0	60	137.0	148.8

Table 9 Variation of combustion irreversibility with bmep at part load, 2000 rpm

Speed (rpm)	ϕ	θ_b (^oCA)	θ_o (^oCA bTDC) (MBT)	p_{in} (kPa)	$p_{exh\ manifold}$ (kPa)	bmep (kPa)	bsfc (g/kW-h)	Destruction of exergy due to combustion (%)
2000 (throttled)	1.0	60	22.5	54	103.4	168.4	397.7	21.30
2000 (throttled)	1.0	60	22.5	75.4	105.0	431.7	285.8	20.97
2000 (throttled)	1.0	60	22.5	94.4	113.9	697.4	260.3	20.87
2000 (Turbo)	1.0	60	22.5	108.3	123.0	886.4	249.8	20.75
2000 (Turbo)	1.0	60	22.5	123.9	136.1	1041.1	245.9	20.64
2000 (Turbo-Full load)	1.0	60	24	137	148.8	1155.9	244.0	20.54

Figure 12 is the plot of combustion irreversibility as a function of bmep at part load. For part loads at 2000 rpm, the turbocharger starts operating after the bmep value of 698 kPa. Thus the graph shows the point where turbocharger becomes active. Overall, the combustion irreversibility values decreased throughout the load range.

The combustion irreversibility values decreased steadily at first with higher bmep values. Once the turbocharger became active, the rate of decrease of values increased slightly. This decrease in values can be attributed to higher pressures in cylinder and a rise in maximum temperatures inside the engine cylinder.

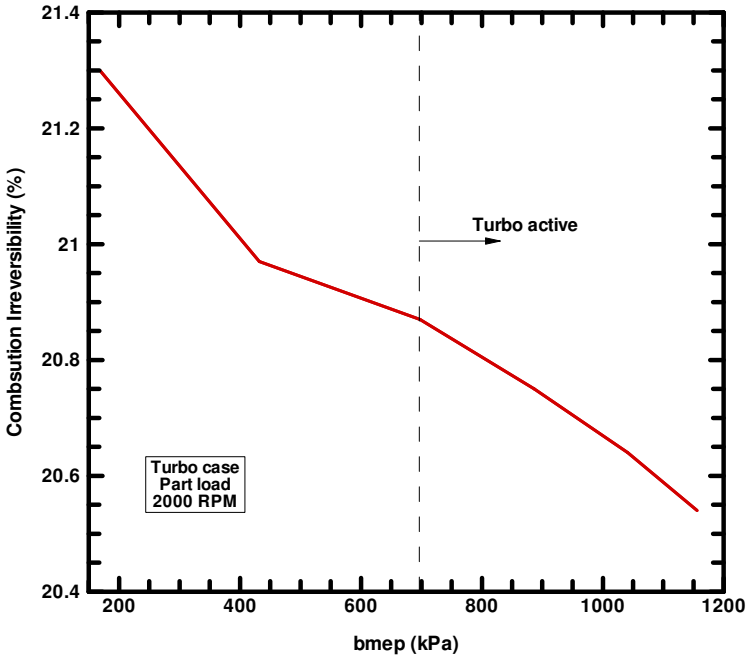

Fig. 12 Combustion irreversibility as a function of bmep for part load, 2000 rpm

d) Variation of effectiveness of intercooler

A simulation study was also conducted in order to investigate the influence of effectiveness on the engine operating characteristics. The brake thermal efficiency and the indicated thermal efficiency of the engine were varied as a function of

isentropic efficiencies of the turbine and the compressor for a specific value of effectiveness. Then, the same calculations were performed for different values of effectiveness. Table 10gives the results for this study. The component efficiency values and effectiveness values in Table 10 were provided as an input. The thermal efficiency values were obtained from the simulation for the base case.

Table 10 Brake and indicated thermal efficiency as a function of isentropic component efficiency, base case, 2000 rpm, WOT

Effectiveness	Comp/Turbine efficiency (%)	Brake Thermal efficiency (%)	Indicated thermal efficiency (%)
0.4	40	32.08	35.5
	50	32.95	35.58
	60	33.04	35.64
	70	33.11	35.68
	80	33.16	35.71
	90	33.21	35.74
0.6	40	33.05	35.64
	50	33.14	35.7
	60	33.21	35.74
	70	33.25	35.76
	80	33.29	35.79
	90	33.32	35.81
0.8	40	33.29	35.79
	50	33.34	35.82
	60	33.37	35.84
	70	33.39	35.85
	80	33.41	35.86
	90	33.43	35.87

Figures 13 and 14 present the thermal efficiency plots as functions of component isentropic efficiencies. For each effectiveness value a graph was plotted and hence

each plot has three graphs. The effectiveness value on top of each graph indicates the same. The brake thermal and indicated thermal efficiency values increased steadily in almost linear manner with an increase in the isentropic efficiency of the components. The reason is that with the higher component efficiencies the irreversibilities associated decrease resulting in improved performance. The same phenomenon was observed for higher values of effectiveness. Higher values of effectiveness also signified that the exergy destruction due to the intercooler heat transfer was reduced and led to an increase in the efficiency.

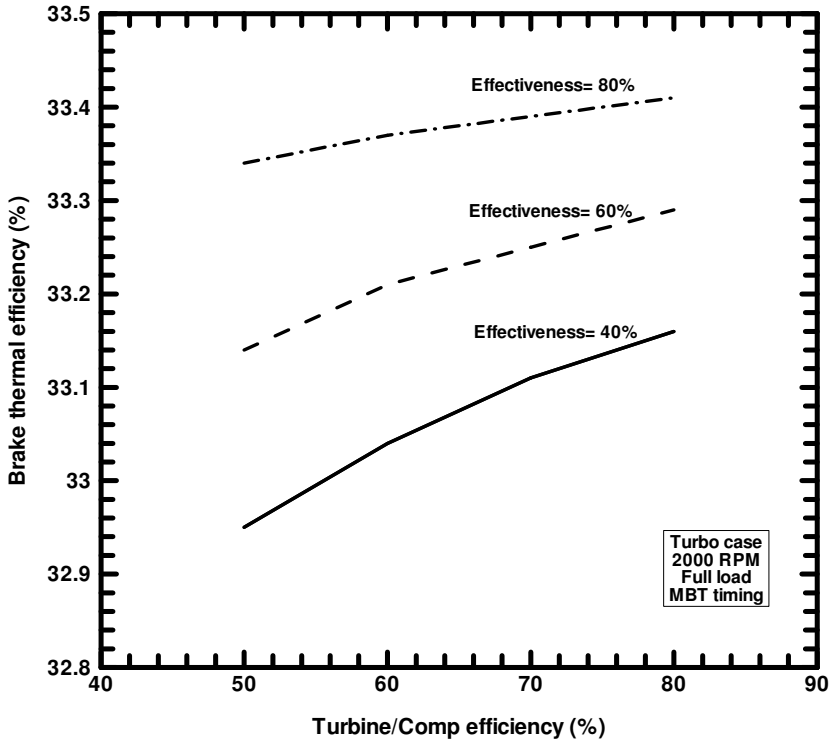

Fig. 13 Brake thermal efficiency as a function of isentropic component efficiencies for varying effectiveness of the intercooler

Figure 14 shows the plot of Indicated thermal efficiency as a function of isentropic component efficiencies. The plot is similar to the brake thermal efficiency plot with effectiveness value being indicated on top of each graph but the values for indicated thermal efficiency are higher.

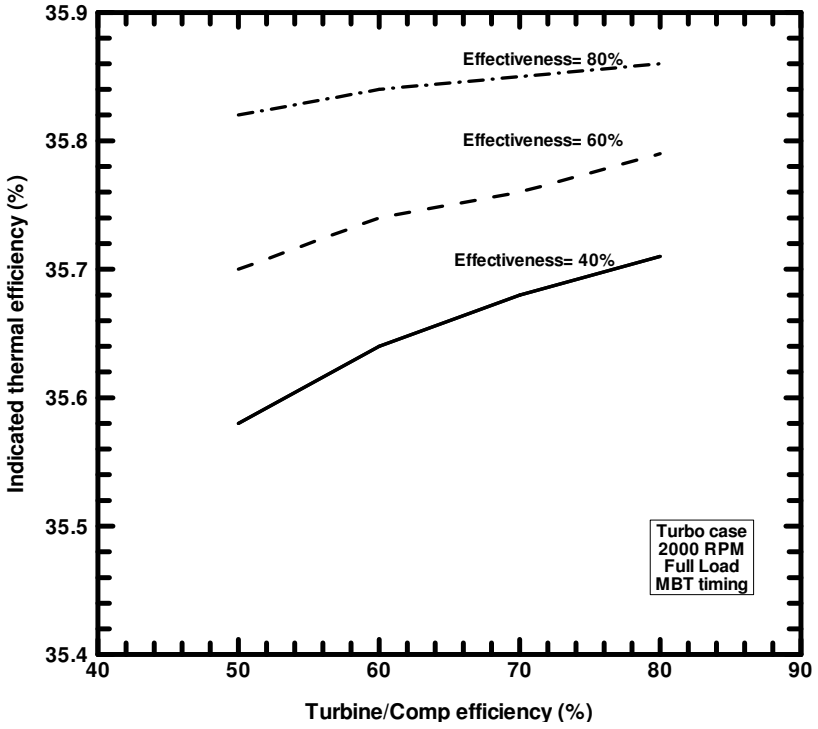

Fig. 14 Indicated thermal efficiency as a function of isothermal component efficiencies for varying effectiveness of the intercooler

Also, an additional simulation study was performed to examine the effects of coolant temperature and effectiveness of intercooler on maximum pressure and fuel consumption of engine. The study was conducted at 2000 rpm, WOT.

The coolant temperature was held at a constant value and effectiveness value of intercooler was varied from initial value of zero to a hypothetical value of one in steps. The values of maximum pressure, bmep and bsfc were obtained from the simulation for each value of effectiveness. Then the same calculations were repeated for different values of coolant temperature. Table 11 lists the input parameters held constant for this entire study.

Table 11 Input parameters for the effectiveness study

Speed (RPM)	**MBT** (°CA)	**P_{in}** (kPa)	**P_{exh}** (kPa)	**T_{in}** (K)	**Eq.Ratio** Φ
2000	-23.0	137.0	148.8	310.3	1.0

Table 12 lists the actual results from this study. The coolant temperature and effectiveness are input parameters and maximum pressure, bmep and bsfc are the output values.

Table 12 Variations in maximum pressure, bmep and bsfc with effectiveness at 2000 rpm, WOT

T_{cool} (K)	**Effectiveness**	**P_{max}**	**Bmep (kPa)**	**Bsfc (g/kW-hr)**
	0	5144.2	1064.7	247.2
	0.25	5290.4	1109.4	245.5
300	0.50	5447.6	1157.5	243.8
	0.80	5660.5	1222.9	241.7
	1	5808.8	1268.3	240.4
	0	5144.2	1064.7	247.2
	0.25	5231.9	1091.5	246.2
320	0.50	5323.6	1119.5	245.1
	0.80	5439	1154.9	243.9
	1	5527.0	1181.9	243.0
	0	5144.2	1064.7	247.2
	0.25	5175.1	1074.2	246.9
340	0.50	5206.4	1083.7	246.5
	0.80	5244.7	1095.4	246
	1	5270.6	1103.3	245.7

Figure 15 displays the rise in maximum pressure with increasing effectiveness of the intercooler. The solid lines indicate maximum pressure and dotted lines indicate bsfc values. The maximum pressure values increased linearly and bsfc values decreased in a linear fashion as well.

This clearly demonstrates the effect of coolant temperature in association with the effectiveness of intercooler on the maximum pressure. An increase in the effectiveness of the intercooler implies better cooling of hot compressed air and thus an increase in the density of the intake mixture and correspondingly an increase in the peak cylinder pressure [16].

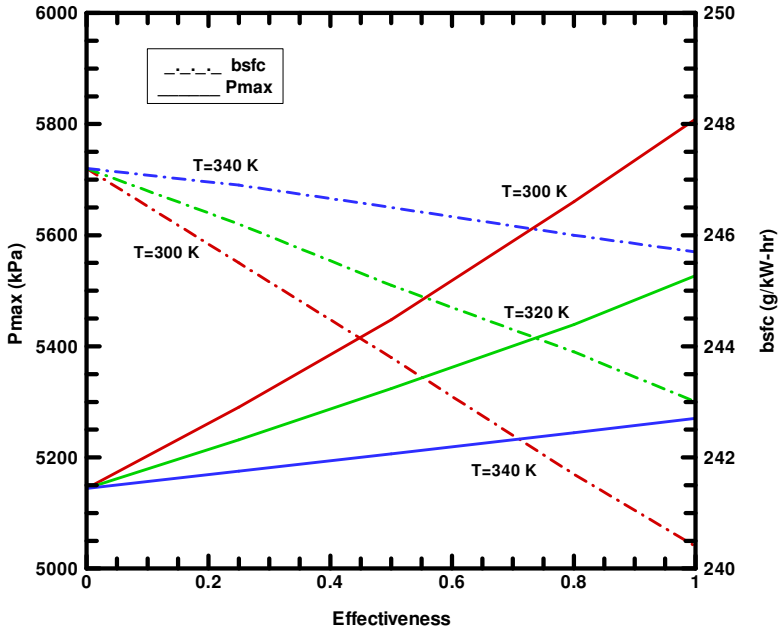

Fig. 15 Variations of the maximum pressure and bsfc with effectiveness and coolant temperature 2000 rpm, WOT

On the other hand, the higher coolant temperature reduced the rise in maximum pressure. Assuming the temperature of hot compressed gas remains the same, higher coolant temperature will reduce the effectiveness of the intercooler. Thus, for the highest value of coolant temperature (340 K), the lowest maximum pressure was

observed. Also, higher density of intake temperature signifies better combustion and lower fuel consumption. This was evident with the plot of bsfc yielding lower values for higher intercooler effectiveness. Considering the above mentioned phenomenon, lower coolant temperature is beneficial for better fuel consumption which is clear from the plots of bsfc (Figure 15). The lowest values of bsfc were observed for lower coolant temperatures.

Figure 16 displays the variations in bmep with the coolant temperature and the effectiveness. Bmep values are indicated by solid lines and dotted lines indicate bsfc values. As, bmep values are a direct consequence of maximum pressure values, the trends for bmep are similar to the maximum pressure but with lower values. However, higher effectiveness values in practice are difficult to achieve due to small temperature differences between the compressed air and the coolant[16]. Thus, a conservative value of 0.6 was employed for most of the calculations.

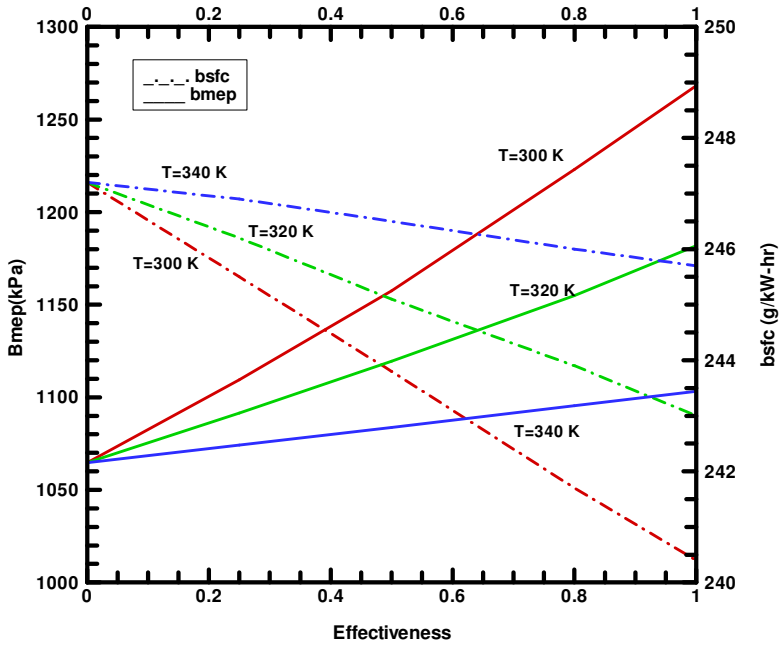

Fig. 16 Variations in bmep and bsfc with varying of intercooler effectiveness at 2000 rpm, WOT

e) Exhaust exergy studies

The turbine of the turbocharger unit utilizes the exhaust energy to drive the compressor which otherwise is released to the ambient. A set of calculations were performed to measure how effectively the turbine exploits the exhaust energy. The study was done for part load operation and for WOT conditions as well.

Table 13 presents the values for part load conditions. The schedule for part load operation (Table 8) was again employed for the computations. Exhaust energy values as a percentage of fuel energy and exhaust exergy values as a percentage of fuel exergy are listed as a function of bmep (kPa).The exhaust energy and exhaust exergy values were calculated at the exhaust port and at the turbine exit for comparison.

Table 13 Exhaust energy and exhaust exergy values as a function of bmep for part load operation

No.	Speed (RPM)	Bmep (kPa)	Exhaust port		Turbine Exit	
			Exhaust energy %	Exhaust exergy %	Exhaust energy %	Exhaust exergy %
1	2000	163.9	38.39	21.52	38.39	21.52
2	2000	431.7	40.79	23.37	40.79	23.37
3	2000	697.4	41.96	24.24	41.96	24.24
4	2000	886.4	42.88	24.65	41.77	23.56
5	2000	1041.1	43.18	25.1	41.66	23.51
6	2000	1155.9	42.92	25.04	41.06	23.1

During part load operation at 2000 rpm, the turbocharger becomes active after the bmep value of 698 kPa and once turbo starts the results become apparent. Figure 17 presents the plot for exhaust energy as a function of bmep for part load operation. The vertical line indicates the point where turbocharger operation starts. The exhaust energy at turbine exit after that point is indicated by the dotted line. The solid line

indicates the exhaust energy at port exit. Before the turbocharger gets active the exhaust energy values at the port and at the turbine exit coincide.

It is clear that exhaust exergy values are lower than exhaust energy values. As, exhaust gases leave the system in a high temperature state and at ambient pressure, they have higher entropy. Thus, from equation 2, the overall exergy for the exhaust flow is reduced [1].

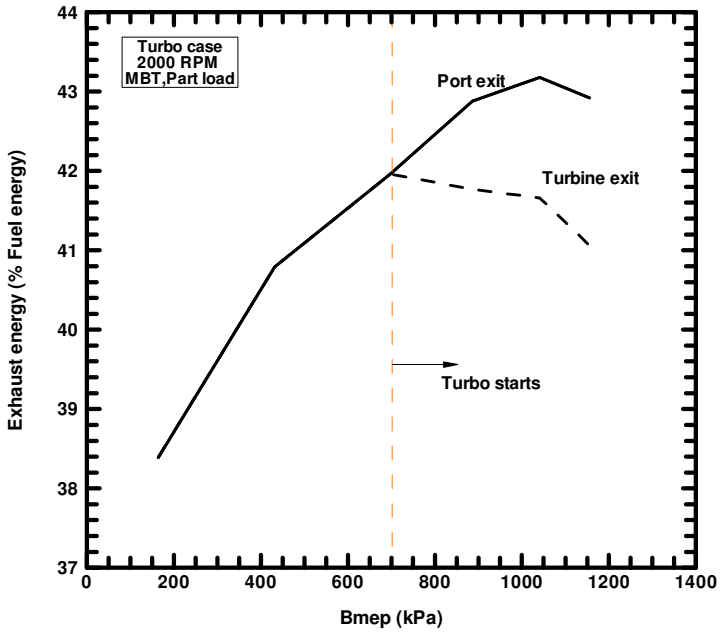

Fig. 17 Exhaust energy (% fuel energy) as a function of bmep (kPa), for part load operation, 2000 rpm

Once the turbo came into effect, the exhaust energy at turbine exit started decreasing with increasing load. The turbine utilizes a part of the exhaust energy and thus less is released to ambient.

Similarly, Figure 18 displays the plot of exhaust exergy as a function of bmep for part load operation. The plot is similar to Figure 17. Dotted line indicates the exhaust exergy values at turbine and solid line indicates exhaust exergy values at port exit. Results showed that exhaust exergy at turbine exit decreased once the turbocharger

became active. The values of exhaust exergy are considerably smaller than the exhaust energy values. The same reason as Figure 17 can be used to explain the results for exhaust exergy values as well.

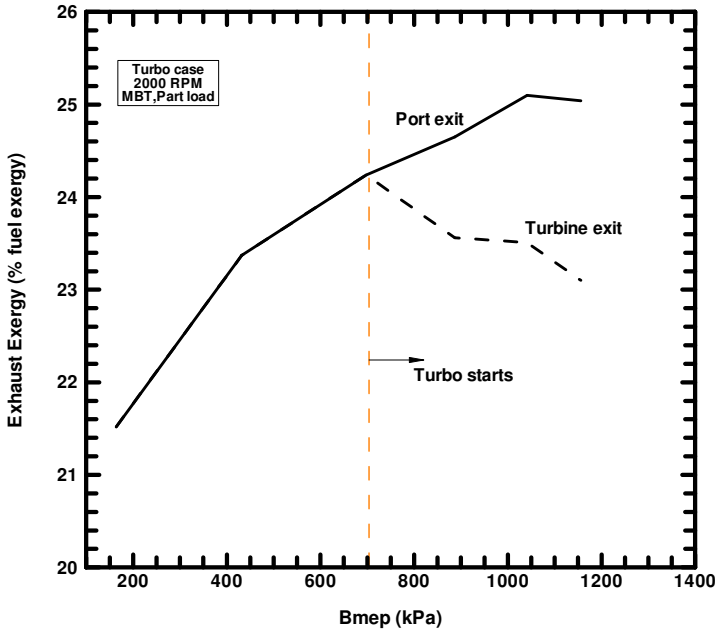

Fig. 18 Exhaust exergy (% fuel exergy) as a function of bmep (kPa) for part load operation, 2000 rpm

Table 14 gives values for the WOT condition. The exhaust exergy and exhaust energy values as functions of bmep over the entire speed range for WOT, are listed in Table 14.These results are quite similar to the part load condition. The schedule for base case from Table 4 was employed to compute the exhaust energy and exergy values.

Figure 19 presents the graph of exhaust energy (% fuel energy) as a function of load for WOT conditions. Exhaust energy values at port exit are indicated by solid line and dotted line indicates the exhaust energy values at turbine exit.

The trends that emerged are quite interesting. Value of exhaust energy continually increased throughout the entire range with increasing load. After the engine reached half of the entire range that is around 2500 rpm, the value of bmep started decreasing.

But the exhaust energy values continued to increase and a sharp rise was observed for latter values. This sharp rise can be attributed to the higher friction mean effective pressure and higher exhaust manifold pressures. Friction mean effective pressure almost linearly increases with the engine speed. Thus, at higher engine speeds even though bmep values decrease, the above two factors cause a sharp rise in exhaust energy and exhaust exergy values.

Table 14 Exhaust energy and exhaust exergy as a function of bmep for WOT conditions

			Exhaust port		Turbine Exit	
No.	**Speed (Rpm)**	**Bmep (kPa)**	**Exhaust energy %**	**Exhaust exergy %**	**Exhaust energy %**	**Exhaust exergy %**
1.	1000	638.9	37.97	20.56	37.01	20.15
2.	1200	754.5	39.78	22.11	38.67	21.32
3.	1500	907.6	41.47	23.61	40.13	22.38
4.	2000	1155.9	42.92	25.04	41.06	23.1
5.	2500	1467.1	44.52	26.62	42.05	23.87
6.	3000	1350.2	45.14	27.11	42.72	24.43
7.	3500	1319.5	45.85	27.71	43.48	25.06
8.	4000	1313.3	46.47	28.22	44.11	25.55
9.	4400	1310	47.25	28.84	44.93	26.16

Unlike the part load operation, for the WOT conditions, turbocharger was active throughout the entire range of the study. The turbocharger utilizes a portion of the exhaust energy. Thus, the values of exhaust energy and exhaust exergy at turbine exit are always lower than the port exit. Also, because of the same phenomenon, the values for port exit and turbine exit do not coincide at any point. Thus, exhaust energy curve at turbine exit follows the curve of exhaust energy at port exit.

Figure 20 displays the plot of exhaust exergy (% of fuel exergy) as a function of bmep for WOT. Again, for exhaust exergy the trends were similar but values of exhaust exergy were lower. The above mentioned concept explains the results of exhaust exergy values as well.

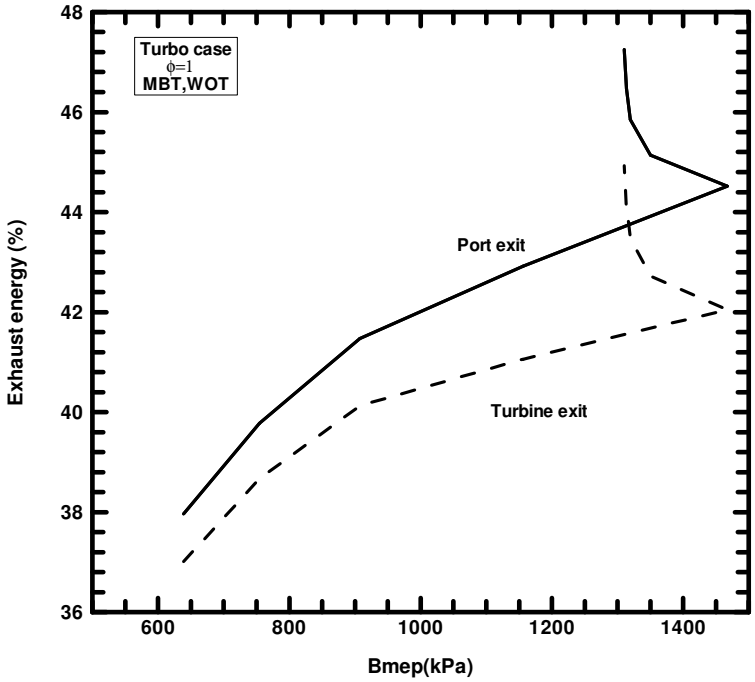

Fig. 19 Exhaust energy (%fuel energy) as a function of load for WOT conditions

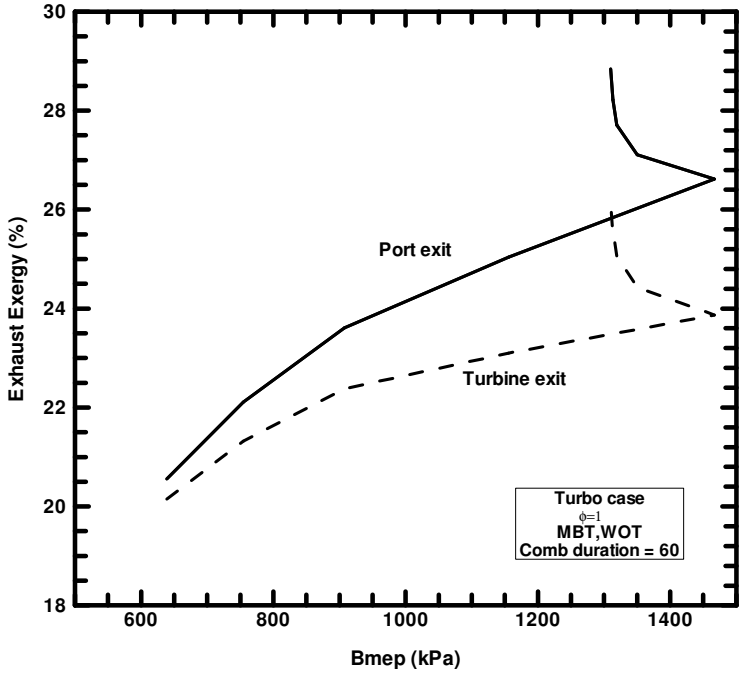

Fig. 20 Exhaust exergy (% fuel exergy) as a function of bmep (kPa) for WOT conditions

f) Varying inlet pressure study

Another simulation study was also performed to investigate the effect of increasing inlet pressure for the turbocharged engine. Figure 6 shows the inlet and exhaust pressure as functions engine speed. For this study, the inlet pressure was not limited but was extrapolated to follow the exhaust pressure curves from Figure 6. When compared with the original schedule, it is evident that the increasing boost pressure increases bmep continuously. Since the maximum pressure also continues to increase, these higher inlet pressures could prove to be detrimental to the engine.

Table 15 gives the new schedule with increasing inlet pressure. Identical to Table 4, Table 15 lists the values of bmep and bsfc as functions of engine speed for the new schedule. The study helped in illustrating the adverse effects of increasing inlet pressure. Thus by not selecting this schedule the higher bmep and consequently higher pressures were avoided.

Table 15 Base case with varying inlet pressure schedule, WOT

Speed (rpm)	ϕ	θ_b (^oCA)	θ_o (^oCA bTDC) (MBT)	p_{in} (kPa)	$p_{exh\ manifold}$ (kPa)	bmep (kPa)	bsfc (g/kW-h)
1000	1.0	60	20	100.0	111.1	638.9	273.1
1200	1.0	60	20	105.2	115.3	754.5	262.7
1500	1.0	60	21	114.7	124.5	907.6	253
2000	1.0	60	24	137.0	148.8	1155.9	244
2500	1.0	60	24	167.7	179.6	1467.1	237.8
3000	1.0	60	24.5	193.0	205.0	1712.9	235
3500	1.0	60	25.0	210.0	219.4	1887.4	234
4000	1.0	60	25.5	219.0	226.0	1977.8	234.5
4400	1.0	60	26.0	222.0	228.3	1995.2	235.8

g) Effect of compression ratio

The engines many times suffer from abnormal combustion. It is the combustion process where flame front is started by hot combustion chamber surfaces either prior or after spark ignition[1]. Knock is one of the forms of abnormal combustion wherein the spontaneous ignition of a portion of end-gas occurs leading to a noise through the engine structure [1]. The noise is called Knock. This abnormal combustion causes very high local pressures and pressure waves propagating across the combustion chamber[1]. In all cases, efforts are made to avoid or minimize the abnormal combustion.

Often, for the turbocharged engines effective compression ratio is lowered. Mainly, to reduce the mechanical and thermal loads induced due to higher operating pressures and also to reduce the peak cylinder pressures, and to avoid the onset of knock [16]. A detailed study was performed to examine the effects of compression ratio on various

parameters like thermal efficiency, combustion irreversibility, etc. For this study the varying inlet pressure schedule was employed. With the above schedule in place, the value of compression ratio (CR) was varied in steps, and at each step, values of thermal efficiencies, bsfc, bmep, maximum pressure and availability destroyed due to combustion were obtained from the simulation.

Table 14 lists initial values of this study along with input parameters. In Table 14, CR, inlet and outlet pressures were the input parameters. Thermal efficiencies, combustion irreversibilities, bmep and bsfc were computed from the simulation.

Table 16 Effect of variation in compression ratio on various parameters for base case with varying inlet pressure, WOT

CR	P_{in} (kPa)	Pmax (kPa)	Brake Thermal Efficiency (%)	Indicated Thermal Efficiency (%)	Bmep (kPa)	Bsfc (g/kW-hr)	Combustion irreversibility (%)
6	100	2419.4	27	30.35	558.7	300.3	21.3
	105.2	2731.3	28.04	31.01	669.7	289.2	21.15
	114.7	3203.2	29.05	31.73	809.3	279.1	21.05
	137	4115.6	30.1	32.48	1044.6	269.4	20.98
	167.7	5260.6	30.86	32.98	1350.3	262.8	20.82
	193	6189.3	31.2	33.21	1594.1	259.9	20.7
	210	6887.2	31.29	33.28	1768.4	259.1	20.62
	219	7302.6	31.17	33.22	1854.2	260.2	20.5
	222	7595.3	30.94	33.1	1868.3	262.1	20.45
8	100	3149.6	29.41	32.97	609.7	275.7	20.96
	105.2	3548.9	30.69	33.85	731.9	264.2	20.79
	114.7	4182.5	31.92	34.77	887.9	254	20.61
	137	5419.7	33.22	35.75	1149	244.1	20.38
	167.7	6962	34.17	36.42	1490	237.3	20.2
	193	8212.6	34.65	36.77	1763.3	234	20.13
	210	9160	34.83	36.92	1960.7	232.8	20.05
	219	9735.1	34.78	36.92	2060.8	233.2	19.98
	222	10187	34.59	36.82	2080.5	234.5	19.92

Table 16 Continued

CR	P_{in} (kPa)	Pmax (kPa)	Brake Thermal Efficiency (%)	Indicated Thermal Efficiency (%)	Bmep (kPa)	Bsfc (g/kW-hr)	Combustion irreversibility (%)
10	100	3835.9	30.72	34.5	639.1	264	20.77
	105.2	4311.4	32.19	35.55	768	251.9	20.55
	114.7	5093.4	33.62	36.64	933.1	241.2	20.34
	137	6663.2	35.13	37.81	1215.1	230.8	20.08
	167.7	8583	36.26	38.63	1577.9	223.6	19.87
	193	10148.7	36.86	39.09	1872.5	220	19.72
	210	11342.2	37.14	39.32	2086.1	218.3	19.63
	219	12077.5	37.16	39.38	2197	218.2	19.56
	222	12701.1	36.99	39.3	2220.3	219.2	19.49
12	100	4491.5	31.34	35.35	654.1	258.7	20.65
	105.2	5043.8	33.02	36.58	789.6	245.6	20.41
	114.7	5966.8	34.62	37.82	960.8	234.2	20.16
	137	7858.2	36.33	39.15	1256.3	223.2	19.85
	167.7	10156.5	37.62	40.11	1636.2	215.5	19.62
	193	12031.8	38.35	40.68	1946.7	211.5	19.46
	210	13459.7	38.71	40.99	2170.7	209.5	19.36
	219	14358.3	38.8	41.11	2290.3	209	19.28
	222	15161.8	38.65	41.04	2316.1	209.8	19.21
14	100	5126	31.57	35.81	659.7	256.9	20.59
	105.2	5750	33.42	37.19	800.2	242.6	20.32
	114.7	6817.4	35.19	38.56	977.4	230.4	20.04
	137	9016.1	37.06	40.02	1280.3	218.8	19.69
	167.7	11699.5	38.51	41.12	1675.6	210.5	19.44
	193	13871.2	39.35	41.79	1995.8	206	19.26
	210	15541.2	39.81	42.71	2229.9	203.7	19.15
	219	16603	39.96	42.35	2356.6	202.9	19.07
	222	17592.5	39.12	42.28	2384.2	203.6	18.98

The objective was to investigate the effect of turbocharging on maximum pressure. Lower compression ratio implies higher inlet pressures (more turbocharging) are possible. Figure 21 shows the maximum pressure as a function of inlet pressure for different values of compression ratio. The value on top of each curve indicates the corresponding compression ratio for the curve. The plot showed that maximum pressures increased almost linearly with an increase in inlet pressure. From the plot, it is also clear that higher compression ratios yield higher maximum pressures. The two dotted horizontal lines indicate the pressures selected for convenience and were used to plot the graphs of different parameters as functions of compression ratio.

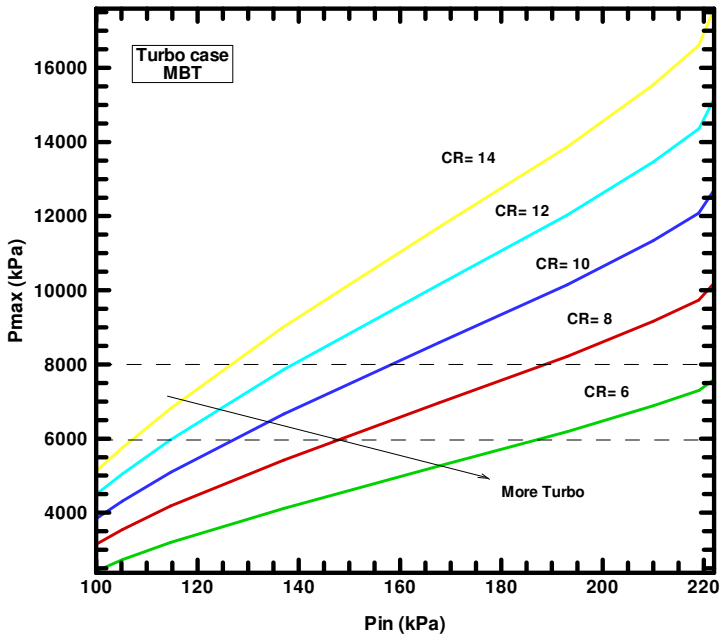

Fig. 21 Maximum pressure as a function of inlet pressure for different compression ratio

To examine the effect of compression ratio on various parameters, a series of graphs were plotted as functions of inlet pressure. Then, using this combined data of compression ratio and inlet pressure values from the plots, the desired graphs were plotted as a function of compression ratio.

Figure 22 shows the thermal efficiencies with varying compression ratio. Both indicated thermal efficiency and brake thermal efficiency are plotted on the same graph. Dotted lines signify the indicated thermal efficiency. The indicated thermal efficiency and brake thermal efficiency both increase quickly for lower inlet pressures up to about 120 kPa, then rise in the values is steady. Overall, the efficiency values showed an increase over the entire range of inlet pressures.

In a similar way, combustion irreversibility was plotted as a function of inlet pressure. Figure 23 shows the plot. The combustion irreversibility curves for different compression ratios are designated by the labels. The curves show a gradual decrease in values throughout the entire range. The drop in the values increases with higher compression ratios.

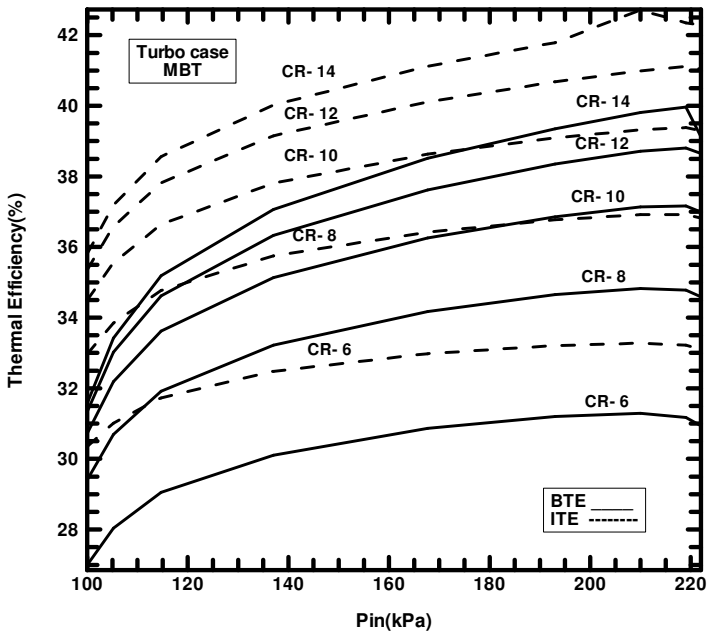

Fig. 22 Brake thermal efficiency and indicated thermal efficiency as a function of inlet pressure for different compression ratio

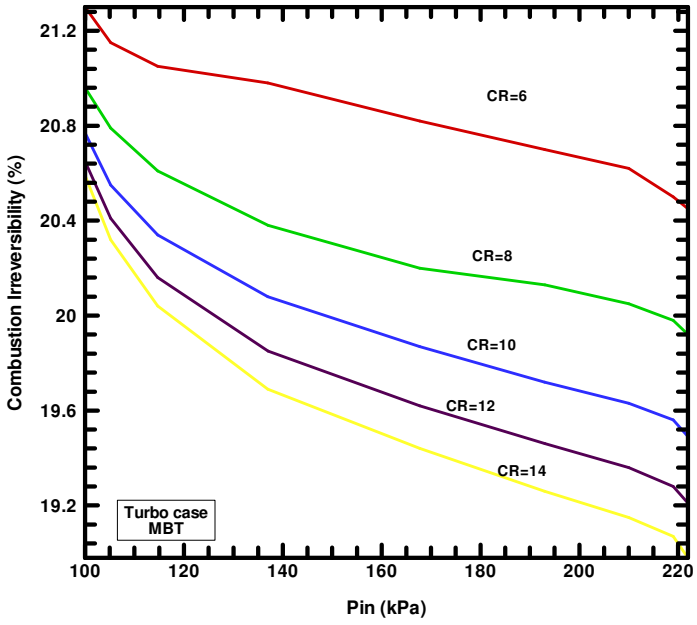

Fig. 23 Combustion irreversibility as a function of inlet pressure for different compression ratio

Following is the plot showing effect of inlet pressure on bmep and bsfc. Figure 24 shows bmep and bsfc as functions of inlet pressure for different compression ratios. Solid lines imply bmep curves and dotted lines signify bsfc curves. Bmep followed the trend of maximum pressure and continued to increase in an almost linear manner with increasing inlet pressure after 120 kPa and the same trends were exhibited with higher values for higher compression ratios. Bsfc values showed gradual drop with increasing inlet pressure. Higher compression ratios yielded lower bsfc values.

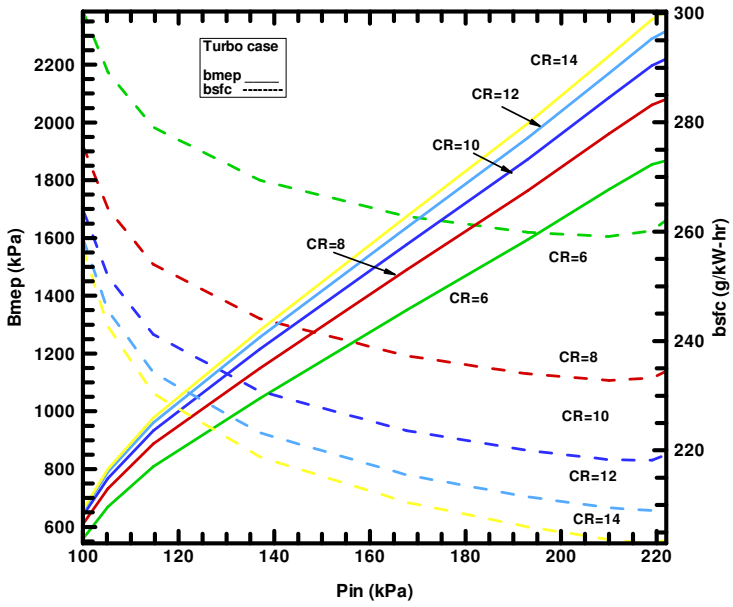

Fig. 24 Bmep and bsfc as a function of inlet pressure for different compression ratio

The objective was to investigate the effect of varying compression ratio on these parameters plotted above. Thus, two pressures 8000 kPa and 6000 kPa were selected as mentioned earlier. To obtain data points for the graphs as functions of compression ratio, following method was employed.

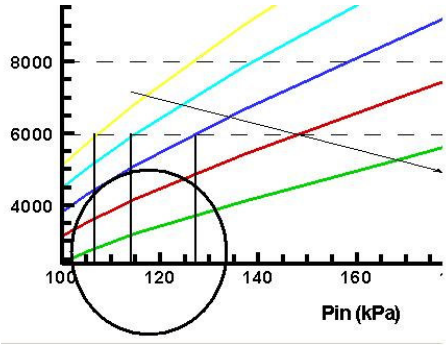

Fig. 25 Method to obtain the performance parameters

Figure 25 is an enlarged section of Figure 21. As shown in Figure 25, the two horizontal pressure lines intersect the compression ratio curves at multiple points. The intersection of the horizontal pressure line and a compression ratio curve gives one inlet pressure point. The vertical lines dropped indicate the corresponding inlet pressure point. Thus for every intersection, one value of inlet pressure was obtained. Now employing these inlet pressure values in Figure 22, the intersection of these points with corresponding compression curve yielded efficiency values as a function of compression ratio. The same process then was repeated for the next set of plots.

Table 17 gives values of inlet pressures obtained using the above method and corresponding values from various plots above. The values are thus functions of both compression ratio and inlet pressure. From these values a series of plots were drawn.

Table 17 Performance parameters as functions of inlet pressure and compression ratio at the constant maximum pressure of 6000 kPa

Speed (RPM)	Pin (kPa)	CR	BTE	ITE	Bmep (kPa)	Bsfc (g/kW-hr)	Combustion Irreversibility (%)
2877.5	186.8	6	31.11	33.15	1534.3	260.6	20.7
2175.7	147.7	8	33.55	35.98	1268.8	241.7	20.3
1766.4	126.5	10	34.42	37.26	1083.3	236.7	20.2
1493.6	114.4	12	34.58	37.79	957.1	234.4	20.2
1259.3	107.0	14	33.76	37.46	853.2	240.2	20.3

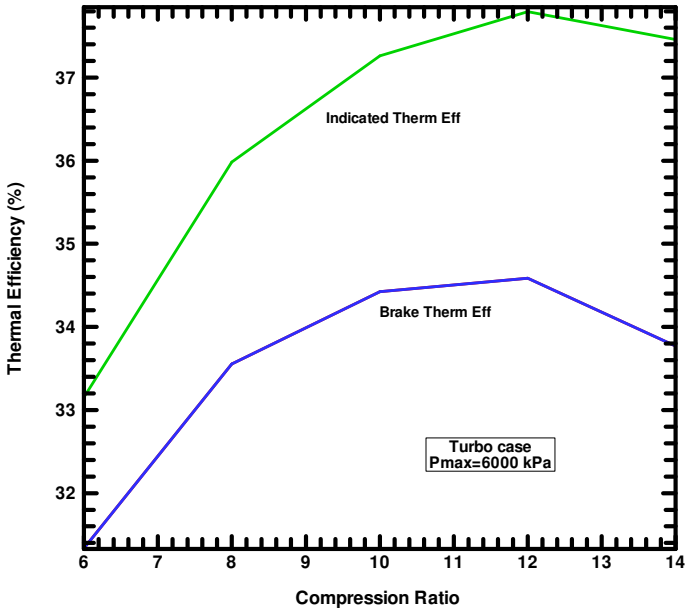

Fig. 26 Indicated and brake thermal efficiencies as a function of compression ratio at the constant maximum pressure of 6000 kPa

Figure 26 displays thermal efficiencies as a function of compression ratio for the reference pressure of 6000 kPa. The thermal efficiency curves showed a steady increase with increasing compression ratios. Curves were identical with indicated thermal efficiency having higher values than brake thermal efficiency.

As, the compression ratio is directly related to the efficiency of Otto cycle, higher compression ratio yields higher efficiency. Also, the indicated fuel conversion efficiency is proven to increase with an increase in the compression ratio [1]. Fuel conversion efficiency is defined as the ratio of work produced per cycle to the amount of fuel energy supplied per cycle that can be released in the combustion process[1]. The indicated fuel conversion efficiency is expressed as equation 15 and is equal to the indicated thermal conversion efficiency as the combustion efficiency has the value of one.

$$\eta_{f,i} = \frac{W_{c,i}}{m_f Q_{LHV}} \tag{15}$$

Thus, higher compression ratios also imply higher thermal efficiencies.

As, values were taken at a reference pressure of 6000 kPa, graphs show a variation. From Table 17, it is clear that for higher compression ratios, value of inlet pressure decreases. This decrease in inlet pressure when employed in graphs to obtain data points creates the disruption. Figure 27 explains this disruption.

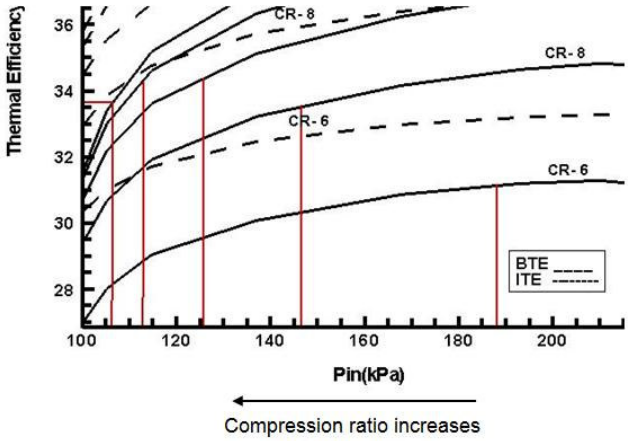

Fig. 27 Graphic illustration of obtaining performance points

Figure 27 is an enlarged portion of Figure 22. The arrow indicates that with increasing compression ratio inlet pressure decreases. From Table 17, for the listed inlet pressures verticals are drawn. For illustration purposes brake thermal efficiency curves are only considered. Thus, the leftmost vertical indicates highest compression ratio (CR=14). From Figure 27, it is clear that for the compression ratio 14, the intersection point of curve and vertical yields lower efficiency value than that of compression ratio of 12. This explains the slight disruption observed in the Figure 26. The same phenomenon was observed in all the graphs.

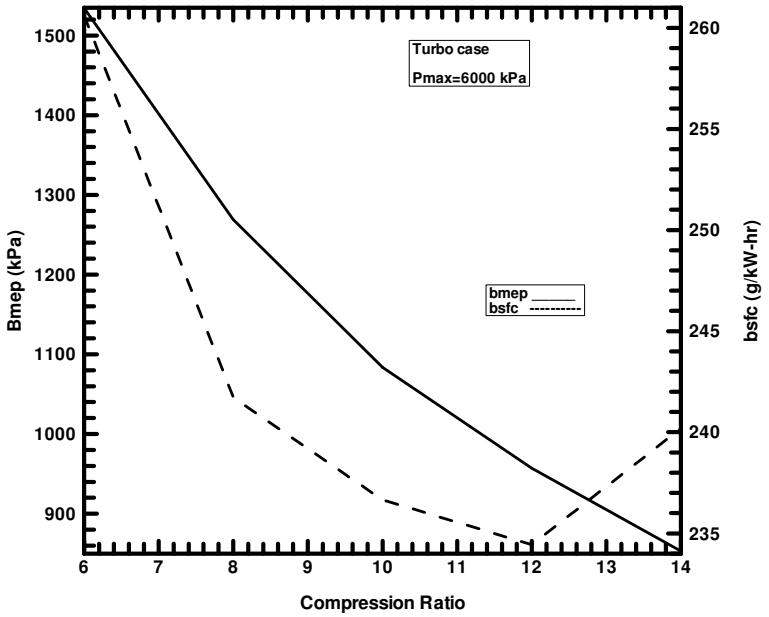

Fig. 28 Bmep and bsfc as a function of compression ratio at the constant maximum pressure of 6000 kPa

Figure 28 shows the behavior of bmep and bsfc with the compression ratio. Bmep values are indicated by solid line and showed a linear decrease with increasing compression ratio. Bsfc values are designated by dotted line and show a sharp decrease with increasing compression ratio.

As mentioned earlier, increase in the compression ratio leads to an increase in the indicated fuel conversion efficiency. Thus, higher fuel conversion efficiency also implies that fuel consumption will be lower. This is confirmed by the plots of bsfc as a function of compression ratio. With an increase in the compression ratio, bsfc values dropped significantly whereas bmep shows a decrease with increasing compression ratio.

Again, as data points are obtained for the constant maximum pressure the bmep values show a different trend. As explained from Figure 27, the values obtained for

bmep display the reverse trend. Bmep values are proved to be increasing with higher compression ratio [1].

Figure 29 is the plot of the combustion irreversibility as a function of the compression ratio. Combustion irreversibility values dropped sharply with high compression ratio. There is a minor deviation for highest compression ratio value due to the trend described earlier.

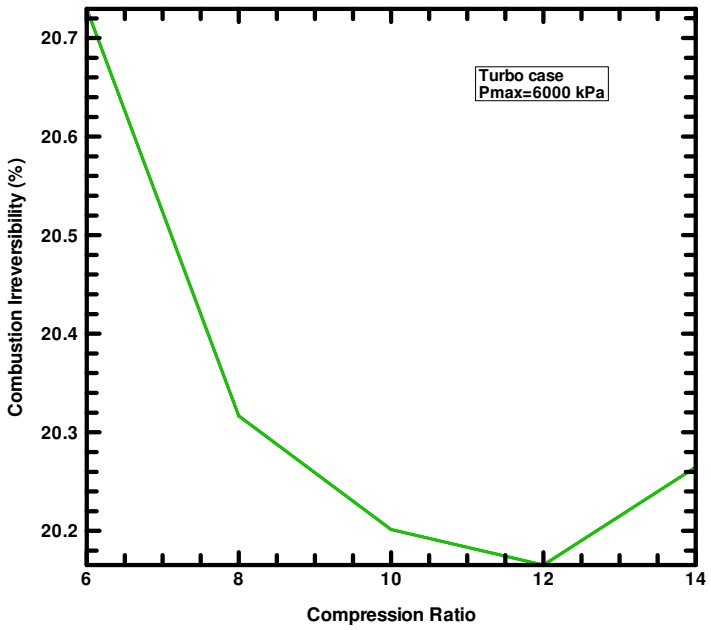

Fig. 29 Combustion irreversibility as a function of compression ratio for a constant maximum pressure of 6000 kPa

The decrease in the combustion irreversibility values can be explained as follows. The higher compression ratios increase the maximum temperature inside the cylinder, which then leads to a decrease in the exergy destroyed. A detailed explanation is given below.

Consider the exergy analysis of combustion process for a constant volume or Otto cycle. The T-s diagram in Figure 30 indicates the processes[1].

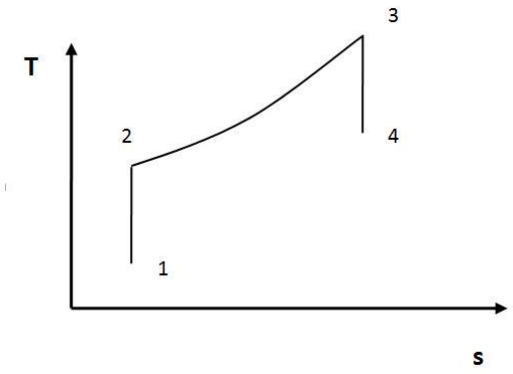

Fig. 30 Temperature-entropy diagram for ideal gas, constant volume cycle

Process 2-3 depicts the combustion process. Exergy analysis of process 2-3 yields, change in exergy for the process 2-3 as [1],

$$\frac{B_3 - B_2}{m_f Q_{LHV}} = -\frac{c_v T_0}{Q^*}\ln(\frac{T_3}{T_2}) = -\frac{c_v T_0}{Q^*}\ln(1+\frac{Q^*}{c_v T_1 r_c^{\gamma-1}}) \quad (16)$$

where,

B_3,B_2 = exergy at state 3 and 2 respectively

T_3,T_2 = temperature at state 3 and 2 respectively

T_0 = Temperature of dead state

c_v = constant volume specific heat

Q^* = the enthalpy decrease during isothermal combustion per unit mass of working fluid

$$= (\frac{m_f}{m_a})Q_{LHV}(\frac{m_a}{m})$$

As the compression ratio increases T_2 increases, and ratio of T_3/T_2 decreases. Thus, from the equation 16, it can be seen that the irreversibility or exergy destroyed decreases with an increase in the compression ratio[1]. This was reaffirmed by the plots obtained in Figure 29. The combustion irreversibility values showed a decrease with increasing compression ratio.

For the maximum cylinder pressure of 8000 kPa, similar approach was followed. The graphs and trends at 8000 kPa were similar to those at 6000 kPa. 6000 kPa has the edge as it also incorporates the compression ratio of 6. Table 18 gives the values for the constant maximum pressure of 8000 kPa as functions of compression ratio and inlet pressure.

Table 18 Performance parameters as functions of compression ratio and inlet pressures for a constant maximum pressure of 8000 kPa

Speed (RPM)	Pin (kPa)	CR	BTE	ITE	Bmep (kPa)	Bsfc (g/kW-hr)	Combustion Irreversibility (%)
2911.1	188.5	8	34.6	36.7	1714.7	234.6	20.1
2344.9	158.2	10	35.9	38.4	1465.4	225.8	19.9
2030.7	138.8	12	36.4	39.2	1279.6	222.7	19.8
1771.2	126.8	14	36.2	39.3	1141.7	224.1	19.8

h) Examining the effect of the boost pressure ratio

Subsequently, a study was conducted at part load to explore the effect of the boost pressure ratio on the engine. The boost pressure ratio is defined as the ratio of the inlet pressure to an engine to the ambient pressure. For turbocharged engines, the inlet pressure is also called boost pressure. For the current study, ambient pressure was assumed to be constant at a value of 100 kPa.

Initially, maximum pressure and maximum temperature as a function of load were plotted at part load at 2000 rpm. Table 19 lists values of the peak pressure and the temperature for the engine cylinder as a function of load. The schedule given in Table 8 was used for the study.

Table 19 Maximum pressure and maximum temperature as a function of bmep at partload,2000 rpm

Bmep (kPa)	Pmax (kPa)	Tmax (K)
168.4	1499.9	2141.2
431.7	2510.8	2294.8
676.4	3446.9	2367.5
886.4	4244.9	2394.3
1041.1	4887.5	2415.8
1155.9	5559.8	2436.8

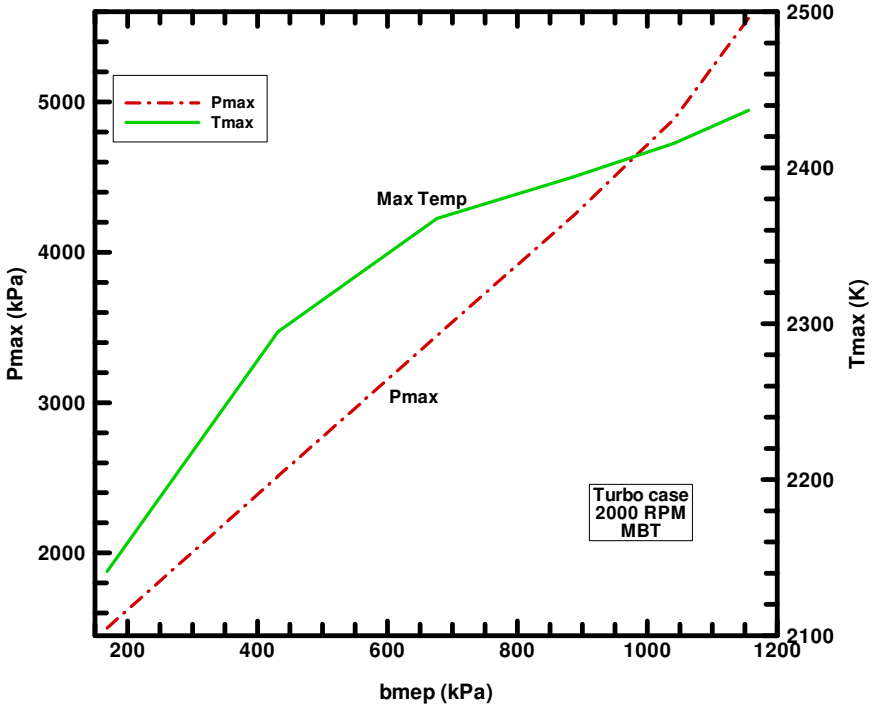

Fig. 31 Maximum pressure and maximum temperature as a function of bmep for part load at 2000 rpm

Figure 31 shows the behavior of the engine peak pressure and the temperature with the engine load. Dotted line indicated peak cylinder pressure and solid line indicated maximum temperature. The peak cylinder pressure increased linearly with an increase in the engine load. Even at part load, the peak temperature increased with

the engine load. Since an increase in the load increases the temperature of the cylinder and combustion chamber walls, temperature of mixture and end gases increases.

Higher boost pressure is desired for turbocharged engines, particularly for enhanced performance. But higher boost pressures also leads to higher pressures and increased chances to the onset of knock. Thus, mostly, the boost pressure is limited by these two factors. Next, keeping other parameters constant at a value, effect of boost pressure ratio (BPR) on the maximum pressure was examined for different compression ratios. Again, the idea was to inspect if turbocharging offers higher boost pressure for the same maximum pressure. Table 20 lists values of maximum pressures for different BPR at a constant value of the compression ratio. For each value of compression ratio, BPR was varied from value of one to two in steps to obtain maximum pressure. Thus for every compression ratio four values of maximum pressure were obtained to facilitate plotting of the curves.

Table 20 Values of maximum pressure as a function of boost pressure ratio for different compression ratio at part load, 2000 rpm

C.R	BPR	Pmax (kPa)
8	1	3485.6
	1.25	4828.0
	1.75	7927.0
	2	8992.7
6	1	2579.0
	1.5	5074.6
	1.75	6082.7
	2	6924.2
10	1	4353.2
	1.25	5976.6
	1.75	9664.7
	2	10943.5

Figure 32 depicts the plots of peak pressure as a function of BPR. The value of compression ratio is indicated on top of each curve. Graphs show almost linear increase in the maximum pressure with higher BPR. Higher values of compression ratio gave higher peak cylinder pressures.

It is important to optimize the compression ratio as to get high BPR within the allowed maximum pressure and also to avoid knock. Figure 32 shows that at any value of maximum pressure, lower compression ratio will yield higher BPR.

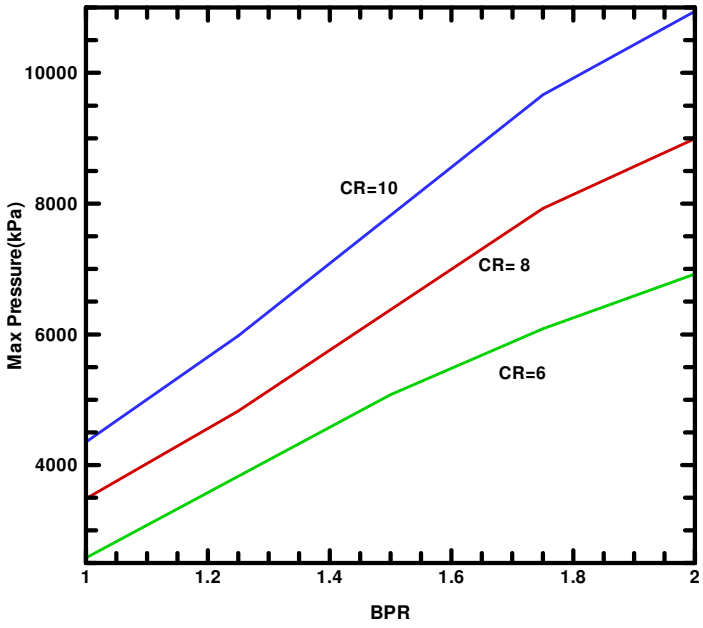

Fig. 32 Maximum pressure as a function of BPR at part load, 2000 rpm

Other operating parameters like bmep and bsfc were also investigated as functions of BPR to examine how BPR affects those. Table 21 gives the value of these parameters as functions of BPR for different compression ratios. The BPR values were varied from value of one to three.

Table 21 Bmep and bsfc as a function BPR at part load, 2000 rpm

C.R.	BPR	Bmep (kPa)	Bsfc (g/kW-hr)
8	1	605.2	273.6
	2	2138.7	221.3
	3	3176.4	213.4
6	1	528.4	306.2
	2	1989.3	243.5
	3	2979.7	234.6
10	1	652.0	257.3
	2	2225.9	209.6
	3	3290.9	202.2

Figure 33 shows the graph of bmep and bsfc as functions of BPR for different compression ratios. The solid lines indicate bmep values and bsfc values are depicted by dotted lines. The bmep values showed linear increase and bsfc values showed linear decrease. The rate of rise of bmep decreased after the BPR value of 2 and similarly, rate of fall of bsfc decreased after the BPR value of 2.

Bmep increased with an increase in BPR. High BPR implies increased air flow. High air flow reduces air/fuel ratio. Thus, weaker air/fuel ratio leads to reduction in brake specific fuel consumption [7].In regards to behavior with compression ratio, as explained earlier it is identical. Higher compression ratio gives higher bmep and lower bsfc. This is significant, as selecting a compression ratio for a better BPR will involve a trade-off. Lower compression ratio will avoid the knock but will yield lower bmep and higher bsfc.

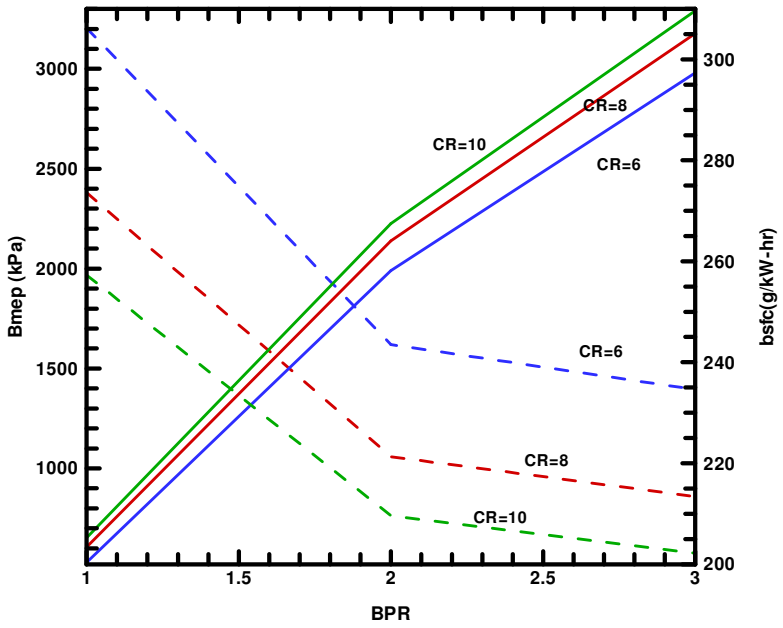

Fig. 33 Bmep and bsfc as a function BPR for different compression ratio at part load, 2000 rpm

5.4.2 Results from the comparative study

A comparative study of the turbocharged engine with the naturally aspirated engine was also performed to get a better insight into turbocharging. Naturally aspirated engines selected for the comparison were a 5.7 liter,V-8 engine and a 3.8 liter,V-6 engine without the turbocharger.

The principal objective of turbocharging is to increase the power output of the engine [7]. The increased density of fuel-air mixture delivered to the engine increases the maximum power. Thus, a smaller turbocharged engine can provide similar maximum power as a larger displacement naturally-aspirated(NA) engine [15].Consequently, a detailed comparative study will help in better understanding of the benefits of turbocharging. Also, one of the objectives was to validate the claims that turbocharging might lead to an efficiency improvement. Table 22 lists results from the comparative study conducted at WOT. The bmep and bsfc values for all three engines

were computed as functions of engine speed at WOT. Inlet pressure for the 3.8 liter, NA engine and 5.7 liter engine was kept constant at 95 kPa. For the turbocharged engine the schedule from Table 4 was employed.

Table 22 Data for comparison of the 3.8 L turbocharged,5.7 L NA and 3.8 L NA engine at WOT

No.		Speed	P_{in} (kPa)	Bmep (kPa)	Bsfc (g/kW-h)
1		1400	95	660.8	264.5
2		2000	95	707.2	257.7
3	3.8L V6 NA	2500	95	718.3	257.3
4		3000	95	713	260
5		3500	95	697.1	265
6		4000	95	673.8	272.1
7		4400	95	648.7	279.5
1		1400	95	870	252.9
2		2000	95	894	247.6
3	5.7L V8	2500	95	894	247.3
4		3000	95	883	249.3
5		3500	95	862.6	253.2
6		4000	95	835.1	258.7
7		4400	95	809.4	264.3
1		1000	100.0	638.9	273.1
2		1200	105.2	754.5	262.7
3	3.8L V6 Turbo	1500	114.7	907.6	253
4		2000	137.0	1155.9	244
5		2500	167.7	1467.1	237.8
6		3000	167.7	1350.2	242.5
7		3500	167.7	1319.5	245.7
8		4000	167.7	1313.3	248.1
9		4400	167.7	1310	250

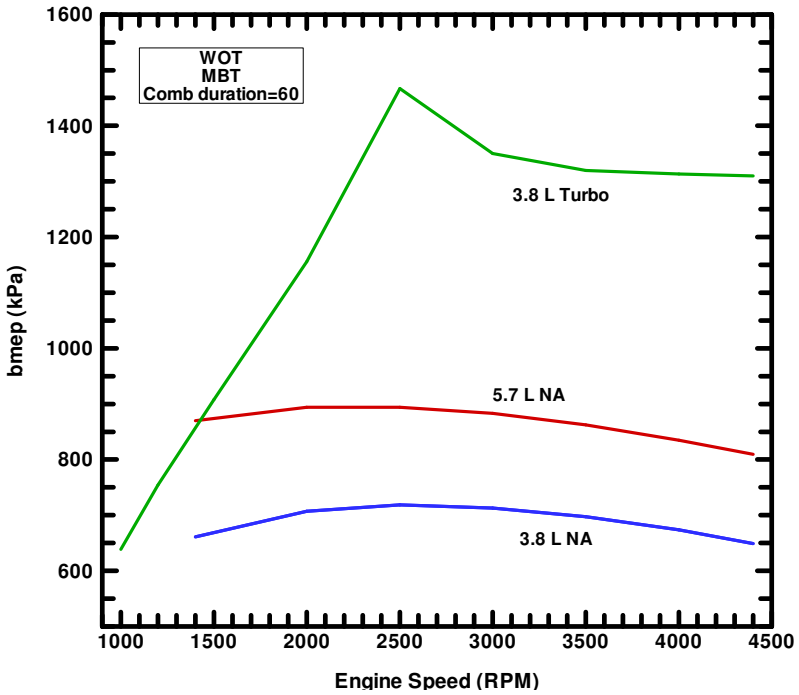

Fig. 34 Comparison of bmep values at varying speeds for all 3 engines at WOT

Figure 34 shows the comparison of bmep for the 3 engines at WOT. The type of the engine is indicated on top of each curve. The bmep values for turbocharged engine increased from low speed to a medium speed of 2500 rpm. The boost control system of wastegate then gets activated to avoid knock. Therefore, the bmep values achieved a steady value for higher engine speeds. The two naturally aspirated engines had bmep values increasing till the engine speed of about 2500 rpm and then dropped gradually. The 5.7 liter engine had higher values than 3.8 liter NA engine. The turbocharged engine clearly benefits from the higher inlet pressure, resulting in higher bmep values than other two engines.

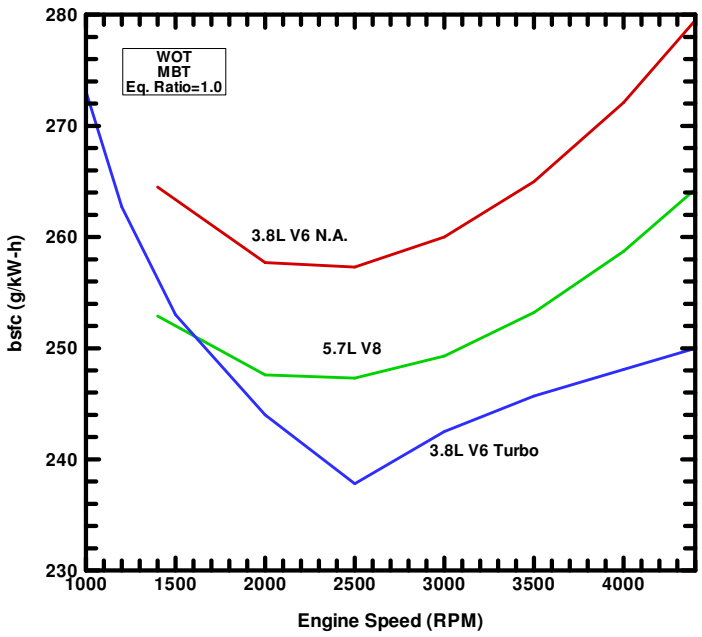

Fig. 35 Comparison of bsfc values at varying engine speeds for all 3 engines at WOT

Figure 35 is the plot showing bsfc values for three engines as functions of engine speed at WOT. Similar to Figure 34, the type of engine is indicated on each curve. The bsfc values for turbocharged engine decreased till about the engine speed of 2500 rpm and then attained steady values. For the two NA engines, bsfc values decreased till about 2500 rpm and then increased slowly for higher engine speeds.

The turbocharged engine offered lowest bsfc values, followed by the 5.7 liter engine and the 3.8 liter NA engine had the highest fuel consumption. As the turbocharger is less effective at very low engine speeds, the fuel consumption was higher than the 5.7 liter engine. The further improvement in the bsfc at slightly higher engine speeds came due to the improved mechanical efficiency [1].

A different study was performed to examine the effect of turbocharging at part load. Turbo is less active at part loads and thus its influence on efficiencies of an engine at part loads is of interest. Table 23 lists values for this study. Employing the part load operation schedule for turbocharged engine (Table 8), a series of values like brake

thermal efficiency (%), brake work (kW), indicated work (kW), etc. were obtained for the turbocharged engine from the simulation. Similarly, same set of values were also obtained for the two NA engines. For the base 3.8 liter engine and 5.7 liter engine, the inlet pressure was increased in steps to 95 kPa.

Table 23 Data for the comparative study of the three engines at part load, 2000 rpm

No.	Engine	MBT (°CA bTDC)	P_{in} (kPa)	P_{ex} (kPa)	Bmep (kPa)	Brake Thermal Efficiency (%)	Indicated Power (kW)	Brake Power (kW)	Total Heat loss (%)
1		22.5	54	104.4	163.9	20.09	15.569	10.708	31.31
2		22.5	75.4	107.4	431.7	28.37	32.489	27.436	24.95
3	**3.8 L Turbo**	22.5	94.4	110.8	697.4	31.39	48.228	43.004	22.45
4		22.5	108.3	123	886.4	32.45	61.718	56.369	21.25
5		22.5	123.9	136.1	1041.1	32.98	71.698	66.210	20.77
6		24	137	148.8	1155.9	33.23	79.110	73.506	20.99
1		20.5	35	102.8	145.6	18.11	20.943	13.987	30.46
2		20.5	40	103.3	205.2	21.35	26.745	19.720	28.06
3		20.5	50	104.4	325.8	25.52	38.487	31.327	25.01
4		20.5	60	105.8	447.06	28.09	50.356	43.060	23.12
5	**5.7 L**	20.5	65	106.5	508.6	29.04	56.293	48.928	22.41
6		20.5	80	109.2	692.3	31.09	74.179	66.610	20.85
7		20.5	85	110.2	777.7	31.79	82.470	74.833	20.15
8		20.5	95	112.4	876.2	32.42	92.086	84.313	19.79
1		22.5	50	104	116.6	16.89	12.242	7.417	34.00
2		22.5	60	105.2	236.1	23.46	19.921	15.007	28.96
3	**3.8 L N.A**	22.5	70	106.5	361.1	27.04	27.954	22.950	26.08
4		22.5	80	108.1	492.4	29.29	36.392	31.297	24.16
5		22.5	90	109.9	632.5	30.85	45.396	40.212	22.73
6		22.5	95	110.9	706.5	31.46	50.151	44.922	22.13

Figure 36 presents the comparison of brake thermal efficiency values for all three engines listed above as function of brake power. The type of engine is indicated next to each curve. The solid line designates the turbocharged engine. The graph shows the

line where turbocharger operation starts as the study is for part load operation. Overall, all three curves showed an increase with the increasing loads. The curves for 3.8 liter, turbocharged engine and the 3.8 liter, NA engine coincide before the operation of turbocharger started. The efficiency values for the 5.7 liter engine are lower than those of 3.8 liter NA engine and but the curve coincides with the turbocharged engine once the turbo gets active.

For lower loads, turbo was not active and consequently, the two 3.8 liter engines performed in the same way. Both 3.8 liter base engine and 3.8 liter turbocharged engine had lower fuel consumption than the larger displacement engine. Thus, for the same load the smaller displacement engines exhibited higher brake thermal efficiency than the larger 5.7 liter engine. Also, the important thing to note over here is the effect of throttling. Due to throttling losses, the brake thermal efficiency values are lower for all the engines. At WOT, respective engines produce maximum brake power. For any values of brake power smaller displacement engines have higher brake thermal efficiency due to lower throttling losses. Also, due to turbocharging the maximum brake power for smaller engine is increased as the WOT point is shifted. Thus, the benefits of downsizing are realized.

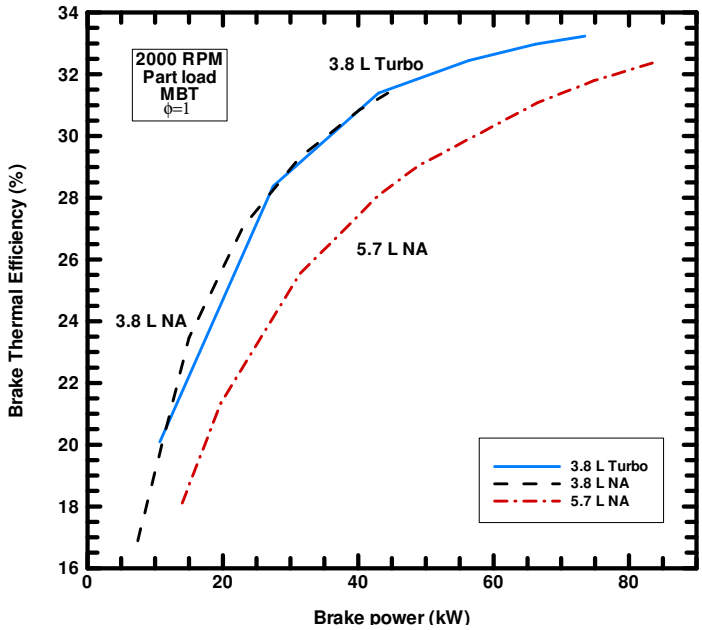

Fig. 36 Comparison of brake thermal efficiency values as a function of brake power for three engines at part load, 2000 rpm

6. SUMMARY, CONCLUSIONS AND RECOMMENDATIONS

A thermodynamic simulation of a turbocharged, four-stroke spark-ignition engine has been used to study the effects of turbocharging from both a first law and second law perspective. A previously developed simulation was modified to incorporate a turbocharger. A detailed exergy analysis of turbocharger components was performed. The exergy associated with the turbine, the compressor and the intercooler was quantified as a percentage of fuel exergy. The study was principally focused on analysis of turbocharged engine. In addition, the thermal efficiency and other operating parameters were determined at part load and for a complete speed range. The main study featured investigating effects of various parameters like compression ratio, intercooler effectiveness, boost pressure ratio, etc. on the operation of the turbocharged engine over the complete load and speed range and also at part loads. The results were in good accordance with the theory.

The results of this simulation study may be summarized as follows:

1) The addition of turbocharger introduces new exergy destruction terms namely the exergy destroyed due to the turbine, the compressor and due to the exhaust flow. Yet, the combustion process remains the largest factor in the exergy destruction. In comparison to exergy destroyed due to combustion, newly introduced exergy destruction terms are considerably smaller. Thus, turbocharging does not contribute considerably to overall irreversibilities.

2) Exergy destruction due to the turbine is always lower than the exergy destruction term due to the compressor. Both the above terms are sensitive of the isothermal efficiencies of the respective components. Increasing the isothermal component efficiency leads to a decrease in the irreversibility associated with the components. Increase in the engine speed increases the exergy destruction terms associated with the turbocharger components.

3) Improved cooling of the hot compressed air increases the density of the intake mixture. Thus, higher intercooler effectiveness yields higher thermal efficiency. In

conjunction with improved component efficiencies, the increase in the intercooler effectiveness results in linear increase in the thermal efficiency. High effectiveness and lower coolant temperature is advantageous for improved performance.

4) The exergy associated with the exhaust is always lesser at turbine exit than at the port exit. Over the complete load range, both exhaust energy and exhaust exergy at turbine exit are considerably smaller than that of the port exit. The same is observed at part loads as well.

5) Higher compression ratio results in higher thermal efficiency. Increasing the compression ratio also gives lower bsfc and higher bmep. Combustion irreversibility is also shown to decrease with higher compression ratios. For the same maximum pressure lower compression ratio yields higher BPR. Again, at any value of BPR higher compression ratio results in lower bsfc and higher bmep.

6) In comparison to both the naturally aspirated 5.7 liter and 3.8 liter base engines, the turbocharged engine offers lower fuel consumption and higher bmep values. For part load operation, turbocharged engine is more efficient than the larger displacement 5.7 liter NA engine.

Overall, the study was helpful in giving deeper insights into turbocharging of a spark-ignition engine. One of the major findings of the study, from the second law perspective is the contribution of exergy destruction terms due to the turbocharger components. Also, employing the turbocharger reduces the exergy associated with the exhaust. Selection of compression ratio is also important. As, lower compression ratio is beneficial in preventing onset of knock but will yield higher bsfc and bmep.
The future recommendations from this work are given below:

1) This simulation can be used for future studies in analyzing the turbocharged spark-ignition engine. Now that the platform exists, this simulation can also be modified to incorporate further features and operations. Current study focused only on the steady state operation. Future works can investigate the behavior of the engine during transient operation from second law perspective.

2) For the current study, the equivalence ratio was assumed at a constant value. The effect of varying equivalence ratio on turbocharging can be also explored. The enrichment and weakening of air/fuel ratio has its benefits and drawbacks.

3) In future, the simulation should also include the possibility to examine the parameters as functions of compression ratio directly, keeping other parameters constant over the entire load and speed range.

REFERENCES

1 **Heywood, J.B.** *Internal combustion engine fundamentals*. 1988 (McGraw-Hill International Editions Singapore).

2 **Caton, J.A.** A review of investigations using the second law of theromodynamics to study internal-combustion engines. *SAE 2000 World Congress*, 2000, **01**(1081), 5-9.

3 **Rakapoulos, C.D. and Giakaoumis, E.G.** Second law analyses applied to internal combustion engines operation. *Progress in Energy and Combustion Sciences*, 2006, **32**, 2-28.

4 **Rakapoulos, C.D.** Evaluation of spark ignition engine cycle using first and second law analysis techiniques. *Energy Conversion and Management*, 1993, **34**(12), 1299-1314.

5 **Sonntag, R.E., Borgnakke, C. and Van Wylen, G.J.** *Fundamentals of thermodynamics* 1988 (Wiley, New York).

6 **Bozza, F., Gimelli, A., Strazzullo, L., Torella, E. and Cascone, C.** Steady-state and transient operation simulation of a "downsized" turbocharged SI engine. *SAE Technical Paper Series*, 2007, **010381**, 3-4.

7 **Watson, N. and Janota, M.S.** *Turbocharging the internal combustion engine*. 1982 (Wiley, New York).

8 **Flynn, P.F., Hoag, K.L., Kamel, M.M. and Primus, R.J.** A new perspective on diesel engine evaluation based on second law analysis. *SAE Technical Paper Series*, 1984, **32**, 5-8.

9 **Traupel, W.** Reciprocating engine and turbine in internal combustion engineering. *Proceedings of the International Congress of Combustion Engines*, 1957.

10 **Patterson, D.J. and Van Wylen, G.J.** A digital computer simulation for spark-ignited engine cycles. *SAE*, 1963, **76**, 82-91.

11 **Caton, J.A.** A multiple zone cycle simulation for spark-ignition engines: thermodynamic details. *2001 Fall Technical Conference of the ASME-ICED*, 2001, 2-5.

12 **Duchaussoy, Y., Lefebvre, A. and Bonetto, R.** Dilution interest on turbocharged SI engine combustion. *SAE International*, 2003, **01**, 3-13.

13 Filipi, Z. and Assanis, D.N. Quasi-dimensional computer simulation of the turbocharged spark-ignition engine and its use for 2- and 4-valve engine matching studies. *SAE International*, 1991, **75**, 3-19.

14 Wang, L.-S. and Yang, S. Turbo-Cool turbocharging system for spark ignition engines. *Journal of Automobile Engineering*, 2006, **172**(220), 2-13.

15 Watts, P.A. and Heywood, J.B. Simulation studies of the effects of turbocharging and reduced heat transfer on spark-ignition engine operation. *SAE Technical Paper Series*, 1980, **80**(0148), 0225-0289.

16 Li, H. and Karim, G. Modelling the performance of a turbocharged spark ignition natural gas engine with cooled exhaust gas recirculation. *Journal of Engineering for Gas Turbines and Power*, 2008, **130**, 4-8.

17 Primus, R.J., Hoag, K.L., Flynn, P.F. and Brands, M.C. An appraisal of advanced engine concepts using second law anlaysis. *IMechE/SAE*, 1984, **C440**, 76-78.

18 Bozza, F., Nocera, R., Senatore, A. and Tuccilio, R. Second law analysis of turbocharged engine operation. *SAE Transactions*, 1991, **100**, 547-555.

19 Shyani, R. Utilizing a cycle simulation to examine the use of EGR for a spark ignition engine including the second law of thermodynamics. *Mechanical Engineering*, pp. 20-37 (Texas A&M University, 2008).

20 Woschni, G. A universally applicable equation for the instantaneous heat transfer coefficient in the internal combustion engine. *SAE*, 1967, **67**(0931), 3065-3083.

21 Stone, R. *Introduction to internal combustion engines*. 1999 (SAE International).

VITA

Name: Vaibhav J. Lawand

Address: Texas A&M University, Department of Mechanical Engineering, 3123 TAMU, College Station, TX 77843-3123.

Email: vjtheone@tamu.edu

Education: Master of Science, Mechanical Engineering, December 2009
Texas A&M University, College Station, TX.

Bachelor of Engineering, Mechanical Engineering, January 2007
University of Mumbai, India.

.